CHALMERS
UNIVERSITY OF TECHNOLOGY

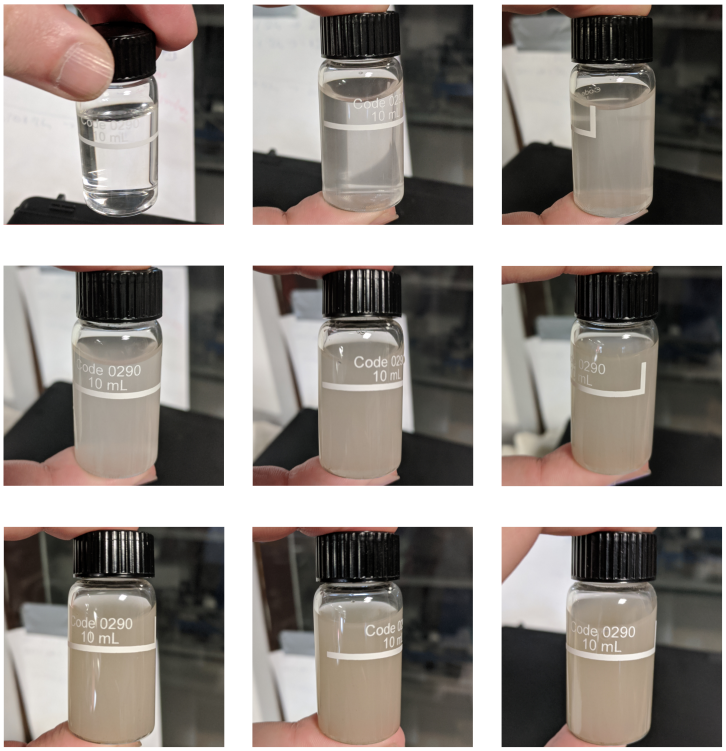

Investigation of optical and ultrasonic measuring techniques for estimation of particle concentration in recycled slurry water

Master's thesis in Systems, Control and Mechatronics

Peter Runneberger
Daniel Karlsson

DEPARTMENT OF ELECTRICAL ENGINEERING
CHALMERS UNIVERSITY OF TECHNOLOGY
Gothenburg, Sweden 2021
www.chalmers.se

Master's thesis 2021

Investigation of sensor and filter combinations for estimation of particle concentration in recycled slurry water

Peter Runneberger
Daniel Karlsson

CHALMERS
UNIVERSITY OF TECHNOLOGY

Department of Electrical Engineering
Chalmers University of Technology
Gothenburg, Sweden 2021

Investigation of optical and ultrasonic measuring techniques for estimation of particle concentration in recycled slurry water
Peter Runneberger
Daniel Karlsson

Supervisor: Christian Nyberg, Husqvarna Construction
Examiner: Torsten Wik, Department of Electrical Engineering

Master's Thesis 2021
Department of Electrical Engineering
Chalmers University of Technology
SE-412 96 Gothenburg
Telephone +46 31 772 1000

Cover: Pictures of concrete slurry samples with different particle concentrations.

Typeset in LaTeX
Printed by Chalmers Reproservice
Gothenburg, Sweden 2021

Investigation of optical and ultrasonic measuring techniques for estimation of particle concentration in recycled slurry water Peter Runneberger
Daniel Karlsson
Department of Electrical Engineering
Chalmers University of Technology

Abstract

A by-product of wet cutting and drilling in concrete is the water an concrete slurry that is created when the concrete dust dissolves in the water. Products exist on the market to manage concrete slurry such as wet vaccum cleaners or other water management systems. Some water management systems reuse the water from the slurry in the cutting and drilling operations by filtering out the concrete particles. When developing new slurry recycling systems, one interesting parameter to monitor is the particle concentration of the recycled slurry. This project compares and evaluates ultrasonic and optical measuring techniques for the estimation of particle concentration in concrete slurry. Three different sensors were used and evaluated during the study. The UB162M4 ultrasonic transducer from PUI Au-dio Inc with a center frequency of 2.47 MHz, using attenuation measurements. The SEN0189 turbidity probe from DFRobot, also using attenuation measurements. The CN0409 sensor card from Analog Devices utilizing both attenuation and nephelometric measurements. The sensors were evaluated by testing them on concrete slurry with a mean particle size of 40 μm and concentrations between 0% to 10% with a focus on concentrations below 2%. The sensors UB162M4 and SEN0189 were also tested on flowing slurry at a constant velocity of 0.62 m/s. On concentrations below 2%, the optical methods outperformed ultrasonic measurements. But when the concentrations reach the point that not enough light penetrates the slurry, ultrasonic measurements outperforms the optical measurement techniques.

Keywords: Turbidity, Ultrasonic, Attenuation, Nephelometric, Particle concentration, Concrete slurry, Slurry recycling, Water quality.

Acknowledgements

We would like to thank the Dust & Slurry team at Husqvarna Construction and especially our supervisor Christian Nyberg at Husqvarna for welcoming us into the team and setting us up for success by introducing us to the right people and helping us acquiring the resources needed to make this project possible. Special thanks also go out to Shreyasu Subramanya for his help with good discussions, purchases and 3D-printing during the project. We also want to thank Torsten Wik for his help during this project.

Peter Runneberger & Daniel Karlsson, Gothenburg, June 2021

Contents

Nomenclature

Acronyms

FAU	Formazin Attenuation Unit
FNRU	Formazin Nephelometric Ratio Units
FNU	Formazin Nephelometric Unit
MMSE	Minimal Mean Square Error
NTU	Nephelometric Turbidity Unit
TSS	Total Suspended Solids
UART	Universal asynchronous receiver-transmitter

Symbols

α	Attenuation coefficient
σ	Attenuation cross section
τ	Optical depth
ε	Molar attenuation coefficient
A	Absorbance
b	Bias in linear model
c	Volume concentration
c_m	Molar concentration
c_n	Number concentration
d	Length between transmitter and receiver
I	Incident light intensity
I_0	Transmitted light intensity
I_{180}	Incident light in attenuation measurements
I_90	Incident light intensity in nephelometric measurements
k_1	Turbidity measurement calibration parameter
k_2	Turbidity measurement calibration parameter
N_A	Avogadro's constant
P_0	Pressure created by transmitter
P_r	Pressure received by receiver
q	Slope in linear model
R	Reflected light
T	Transmittance
V_0	Voltage used to generate transmitted signal
V_r	Voltage generated by received light intensity

1

Introduction

In cutting and drilling operations of concrete, water is often used in order to increase the cutting or drilling power. This water can also be used to collect the concrete dust particles created by the operations. The dust particles, if not collected, are considered a workplace hazard and are harmful to inhale, as explained in [1]. However, when wet cutting or drilling, the dust particles created by the operations are dissolved in the water, forming a slurry and does not end up in the air. This slurry can then safely be vacuumed by wet vacuum cleaners and later disposed of.

Another option to collect and directly discard the slurry is to recycle the water by filtering out the concrete particles. The recycled water can then be reused in the cutting or drilling application, and the rest of the slurry disposed of separately. This recycling method uses less water than the standard non-recycling method. Which is particularly important in regions with dry climate [2].

Combining a battery driven slurry recycling machine with a cordless power tool opens the possibility to perform wet cutting and drilling operations without any wall connections. This does not only decrease the time needed for setup before wet cutting or drilling. It also removes the need for having a water source at the construction site, since you can use the recycle machine as a water source and bring the water needed with you.

The quality of the water that the slurry recycling machine outputs could have great importance for the power tools it is used with. When using recycled slurry water in power tools there are mainly four parameters of water quality that can prove to be harmful to the tool. The four parameters are particle size, particle concentration, temperature and pH. Concrete slurry has a very high pH of around 12, and is caustic and corrosive. In a power tool this means that parts that are not dimensioned to withstand this might start to disintegrate and break down over time. The high pH also complicates the disposal of concrete slurry. If the temperature of the water rises too high, it will start to affect the performance of power tools that utilizes the water for motor cooling. If the size of the particles is too large then they might start destroying pumps, water cooled motors and other parts of the slurry recycling machine or power tools. With a higher concentration, another problem becomes more probable, a build-up of sediment. Build-up of sediment occurs over time but the rate will increase with the concentration of the recycled slurry water.

1.1 Background

The fundamental difference between a slurry recycling machine and a standard wet vacuum cleaner is the slurry filtration system and the water feedback. When designing a filtration system there has to be a balance between flow rate through the system and level of filtration. For example, the rate of slurry that can be filtrated through a system that utilizes a filter bag will be decided by how fine the mesh of the filter bag is, the pressure and the surface area of the filter bag that is in contact with the slurry. A finer mesh will filter slurry at a lower rate, but the filtrated water will have a lower concentration of particles. Both the particle concentration and flow are important parameters for the feedback water. If the flow through the filtration system is too low, it might result in water shortages for the power tools. On the other hand, concrete particles left in the recycled water might cause unnecessary wear on the power tools and might destroy more delicate parts of the machine. If the recycled slurry water dries inside the machine, leftover particles might solidify and sediment will start to build up inside the power tool over time.

The particle concentration is expected to change over time and will reflect the state of the filter bag. Online measurements are more important for particle concentration than for particle size. This is because when the concrete slurry is filtrated through a filter bag then the particle size is limited by the mesh size.

Monitoring water quality is a crucial part for the development of products where recycled water is expected to be used and the quality of the water has an impact on the product. Today Husqvarna relies on sending samples to an external lab. The goal of this project is to develop and investigate different fast and cost effective ways to measure particle concentration in recycled slurry water. The investigation looks at both a solution that could be integrated into a product and used in a more controlled laboratory environment.

1.2 Related work

There are multiple ways to measure particle concentration, such as radioactive [3], electrical [4], optical [5] and ultrasonic methods [6]. The radioactive method has high accuracy but is slow and special care is needed to not be a risk for the operator's health [3]. The electrical method is fast but is easily affected by conductive particles, such as iron particles from reinforcement bars [3]. The optical methods are fast and can achieve high accuracy measurement for lower concentrations of particles [3]. This method becomes less effective as the particle concentration increases and less light is transmitted through the liquid. It is possible to get non-invasive measurements using optical sensors, as long as the sealing is transparent. Ultrasonic methods are fast but the accuracy decreases at lower concentrations. Ultrasonic methods work better than the optical ones when it comes to non-invasive methods and for higher particle concentrations, since the ultrasonic waves can be used through materials that light cannot penetrate. With this in mind, the project

has been limited to testing optical and ultrasonic methods.

1.2.1 Optical measuring techniques

The two most common techniques to estimate particle concentration in fluids found in our study of previous litterateur, are particle counting using lasers [7] and turbidity measurements using LED or tungsten lamps [8]. Particle counting methods using laser are often found in expensive lab equipment and they give a very exact measurement of the particle concentration. Turbidity measurement equipment measures the turbidity instead of the particle concentration. A common way to get the particle concentration from a turbidity measurement is to map a turbidity unit to TSS (total suspended solids) [mg/L] measurement [8].

Of these two techniques, turbidity measurements are the most versatile. It is used both in lab environments and in muddy rivers with minimum maintenance. This versatility has led to the development of a wide variety of measuring standards [8] and equipment in different price classes. For this project, price and robustness have higher priority than a precise measurements, therefor, the only optical techniques investigated are turbidity measuring techniques.

1.2.2 Ultrasonic measuring techniques

There exist multiple different techniques for measuring particle concentration in a medium using ultrasound. One method is based on the assumption that the shape of the energy lobe sent from the transmitter changes when the ultrasound travels through a scattering medium. This method is used in [6] to estimate the mass fraction (0-15%) of iron ore particles with particle size 0-10 μm. To achieve this the authors use one transmitter with a center frequency of 3MHz and two receivers. They show a linear behavior for concentrations above 3%.

Other techniques use one transmitter and one receiver, such as in [9]. The authors then use one transmitter and one receiver with a center frequency of 2.25 MHz to measure the weight percentage of kaolin (aluminum silicate) particles. The kaolin particles have a plate like shape with a mean diameter of 1.04 μm. They perform attenuation measurements through the liquid using frequencies between 0.5-3 MHz and a weight percentage between 3.5 and 44%. They found that the attenuation was a linear function of the particle volume fraction, for any given frequency. They also found that the attenuation has a linear dependency upon frequencies in the interval 0.5 to 3.0 MHz, for a given a particle volume fraction. In [10], one transmitter and receiver is also used. The center frequency of the transmitter and the receiver is 2.5 MHz. The authors use a multi-frequency (1-5 MHz) ultrasound attenuation method to estimate both the particle size distribution and concentration. The medium measured on is acrylic spheres, with a particle size of [1.5, 2.0, 2.5, 3.0]mm and a volume concentration of 5-25%, in saltwater.

Other studies, such as [11] and [12], use only one transducer. In [11], the authors used one transducer with a center frequency of 2.25 MHz and a pulse-echo technique to measure local volume concentration for lime glass particles with a diameter of 180-210 μm. The tests were performed using flow velocities of [1.2, 2.0, 2.5, 3.0]m/s and a volume concentration of 1-10%. This method is based on measurements of backscatter intensity and attenuation. In [12], two independent methods for measuring particle size and concentration in Coal-water slurry, with a weight concentration 45-65% are presented. One method uses a multiple echo reflection method, the other one uses an ultrasonic attenuation spectrum method. Both methods presented in [12] uses a pulse/receiver in combination with a single transducer with a center frequency of 5 MHz.

From the literature presented above, we conclude that the most common choice of center frequency is between 2 and 3 MHz. For measuring the particle concentration, attenuation measurements are common, either using two transducers or using one transducer with pulse-echo techniques.

1.3 Purpose

The purpose of this thesis is to investigate ultrasonic and turbidity measurement techniques in order to determine the particle concentration in recycled slurry water. The solutions are compared and evaluated for use in a test rig for the slurry recycling machine and possible use inside the final product.

1.3.1 Research questions

- What is the expected range of particle concentrations in recycled slurry water?
- How does the different measuring techniques compare based on accuracy?
- Are any signal filters necessary in order to get accurate sensor readings?

1.4 Scope

The particle size distribution of the concrete dust in the water that has been filtrated through a filter bag is currently unknown and varies depending on the filter bag used and is therefore difficult to reproduce. Due to the time limit in this project, all measurements will be done using water mixed with concrete dust particles with a mean diameter of 40 μm acquired from dry cutting.

There exist non-invasive methods for ultrasonic measuring. However, to simplify the problem the sensors will be in direct contact with the medium.

Given the project's limitation in time and budget, only two sensor solutions for turbidity measurements, and one for ultrasonic measurements will be tested. The two

turbidity measurement techniques will use nephelometric and transmittance measurement methods and a combination of these. In nephelometric techniques, the light intensity is measured from a 90° angle relative to the incident light. The ultrasonic measurement will be limited to the use of two transducers and will rely on attenuation measurement techniques.

2
Theory

This chapter will clarify how absorbance is defined in the context of this report and presents the fundamental equations that the methods in this report are based on.

2.1 Absorbance & Transmittance

In optics, transmittance and absorbance are the properties that describe how much of a transmitted light that passes through a medium, and how much that is absorbed. Transmittance (T) is defined as

$$T = \frac{I}{I_0},$$

where I_0 is the intensity of the light entering the liquid and I is the intensity of the light that have passed straight through the liquid.

Absorbance (A) can be defined in different ways. A common way to define absorbance is as a part of the following equation, $T + A + R = 1$. Where T is the transmittance, A is the absorbance and R is the reflected light [13]. However, this is not the definition of absorbance used in Beer-Lambert law and thus not the definition that will be used in this report. In [14], the absorbance used in Beer-Lambert law is defined as the optical density:

$$A = \log_{10}\left(\frac{1}{T}\right).$$

2.2 Beer–Lambert law

A common and practical expression of the Beer–Lambert law relates the absorbance of the sample with its molar attenuation coefficient (ε), molar concentration (c_m) and the optical path length (d) [14]:

$$A = \log_{10}\left(\frac{1}{T}\right) = \varepsilon d c_m. \tag{2.1}$$

According to [15], the optical depth (τ) is defined as

$$\tau = \ln\left(\frac{1}{T}\right),$$

where ln denotes the natural logarithm. If the optical depth is used instead of the absorbance then Equation (2.1) can be rewritten as:

$$\tau = \ln\left(\frac{1}{T}\right) = \varepsilon d c_m \cdot ln(10).$$

The molar attenuation coefficient and the attenuation cross section (σ) are according to [16], related by the following expression

$$\varepsilon = \frac{N_A}{ln(10)}\sigma,$$

where N_A is the Avogadro constant. The molar concentration and the number concentration (c_n) are related by [14]

$$c_m = \frac{c_n}{N_A}.$$

Thus, the optical depth can be expressed as a linear equation of the attenuation cross section, optical path length and the number concentration, according to

$$\tau = ln\left(\frac{1}{T}\right) = -ln\left(\frac{I}{I_0}\right) = \sigma d c_n. \tag{2.2}$$

The volume concentration (c) is proportional to the number concentration and the voltage in the sensor is proportional to the light intensity. Introducing the new variables q and b, where b is correlated to the optical depth of clear water and q is correlating to σ and d, the formula can then be written

$$-q \cdot ln\left(\frac{V_r}{V_0}\right) + b = c. \tag{2.3}$$

Where V_r is the voltage generated by the receiver. In our case $V_0 = 4.5$ is the maximum value from the sensor [17], q and b are calibrated using Minimum Mean Square Error (MMSE).

2.3 Turbidity measurements

One way of measuring water quality is by measuring the turbidity of water. Turbidity sensors measure the light intensity through a medium and they come in different types.

Turbidity measurements describe how transparent the fluid is. The turbidity of a fluid is determined by directing a light through a sample and measuring the intensity of the scattered light at different angles from the light source. The measured light intensities are mapped to different turbidity units depending on the light source and measurement angle. Examples of the units are Nephelometric Turbidity Unit (NTU), Formazine Nephelometric Unit (FNU), Formazin Nephelometric Ratio Units (FNRU) and Formazine Attenuation Unit (FAU) [18, 19]. All modern turbidity units

are based on measurements of a formazine suspension that is produced by mixing solutions of 10 g/L hydrazine sulfate and 100 g/L hexamethylenetetramine. Measurements on this solution are defined as 4000 NTU/FNU/FNRU/FAU [18]. It is also important to note that measurements can vary between different sensors and samples measured upon.

The main differences between the different turbidity units are the light source and the angle at which the light intensity is measured. The common choices of light sources are a tungsten lamp, an IR LED or a near IR LED. The most commonly used measuring angles are nephelometric (90° scatter) and light transmittance by measuring at 180° from the light source. There exist techniques that use backscatter (< 90° scatter) and forward scatter (> 90° scatter). However, these are not that common [8]. A visualization of the different measuring angles can be seen in Figure 2.1.

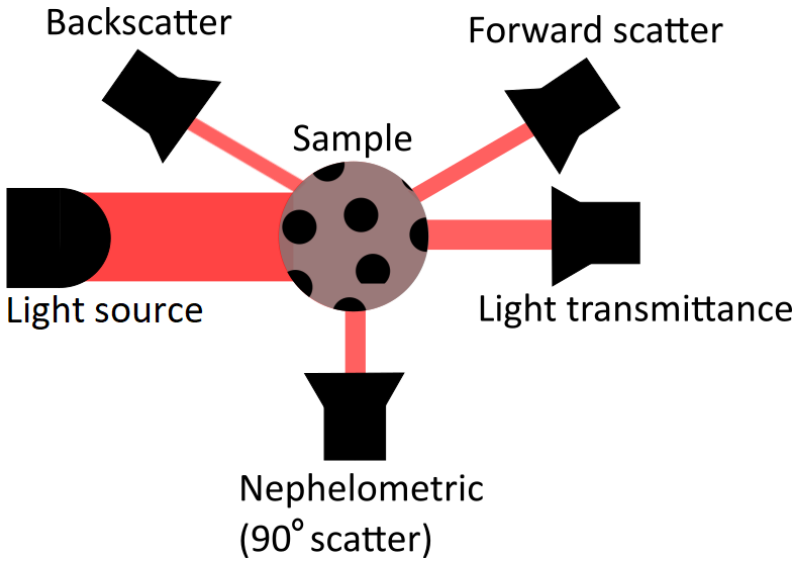

Figure 2.1: Visualization of the different types of turbidity measurements.

Most of the turbidity measurement standards rely on the nephelometric scatter and are limited to the interval 0-40 NTU/FNU, for example, EPA Method 180.1 and Standard Methods 2130B [8]. To measure higher turbidity, the samples need to be diluted. There are, however, standards which use the transmittance measurements. One example is ISO 7027-1:2016, that is defined for nephelometric measurements for concentrations between 0-400 NTU/FNU and transmittance measurements for 40-4000 FAU [19].

2.3.1 Turbidity models

For a low concentration of slurry, the 90° scatter is estimated to behave linearly with respect to the turbidity. This is described in [20] and the relationship can be modeled as

$$Turbidity = k_1 I_{90} + k_2,$$

where k_1 and k_2 are calibration parameters and I_{90} is the light intensity of the 90° scatter. If the light source is near IR and only the 90° scatter is used to estimate the turbidity, then the turbidity is measured in the FNU unit.

When the 180° scatter is used, the properties of Beer–Lambert law can be applied [20]. One way to model this is:

$$Turbidity = -k_l \cdot ln\left(\frac{I_{180}}{k_2}\right),$$

where k_1 and k_2 are calibration parameters and I_{180} is the light intensity of the 180° scatter. If the light source is near IR and only the 180° scatter is used to estimate the turbidity, then the turbidity unit used for the measurement is FAU.

If a combination of different angles of measurements are used and the light source is near IR, then the turbidity unit used becomes FNRU. Since multiple measurements are combined to estimate the turbidity, the number of ways to calculate the turbidity drastically increases. Three examples from [20] of how to model the turbidity using only the 90° scatter and 180° transmittance are

$$Turbidity = \frac{I_{90}}{k_1 I_{90} + k_2 I_{180}},$$

$$Turbidity = \frac{k_3 I_{90} + k_4 I_{180}}{I_{90} + k_2 I_{180}},$$

$$Turbidity = k_1 \frac{I_{90}}{I_{180}} + k_2.$$

These three models will be calibrated on calibration fluids based on different formazin concentrations, as explained in Section 2.3. The result of this is that all models will give a similar estimation of the turbidity when they are used on a formazin solution. However, when the models are used on other solutions (for example coffee or concrete slurry) the models will output different turbidity levels. This is because the relationship between the 90° and 180° measurement differs from the one measured on the calibration fluid.

Since the measured turbidity value differs depending on the medium, the measuring model and the equipment used, it is not recommended to compare different turbidity values taken out of context.

2.4 Ultrasonic attenuation measurements

According to [21], the attenuation of a ultrasonic signal through a medium can be calculated using

$$\text{Attenuation} = ln\left(\frac{P_0}{P_r}\right) = \alpha d,$$

where α is the attenuation coefficient, d is the distance between the transmitter and the receiver, P_0 is the pressure created by the transmitter and P_r is the pressure

measured by the receiver.

Since the pressure is proportional to the voltage in the transducers [9], the equation can also be written as

$$ln\left(\frac{V_0}{V_r}\right) = -ln\left(\frac{V_r}{V_0}\right) = \alpha d. \tag{2.4}$$

The attenuation coefficient (α) is very complex and depend on frequency, thermal effects, scattering effects, visco-inertial effects, intrinsic absorption effects and more [10]. Several studies have however shown a linear behavior of the attenuation coefficient with regard to concentration [9, 22]. To map the relationship between concentration and attenuation the parameters q and b are introduced. The parameter q represents the slope and correspond to αd. While b represents the bias and corresponds to the energy loss in clear water, as well as the loss in the conversion between voltage and pressure. The new equation can be written as

$$-q \cdot ln\left(\frac{V_r}{V_0}\right) + b = c, \tag{2.5}$$

where both q and b will be calibrated using a MMSE estimation.

3
Equipment

In this chapter, the equipment used in the project will be presented and the different choices made regarding sensors and construction of the test rigs will be motivated.

3.1 Choice of electronics and sensors

Many factors affected the choice of electronics and sensors, such as price, delivery time, documentation, measurement quality, available code and the ability to access raw measurement data. The possibility to use the sensors in the slurry recycling machine was also taken into consideration. Two different turbidity sensors and one ultrasonic sensor were evaluated in the project.

3.1.1 Turbidity sensors

Two different sensor solutions for turbidity measurements were tested: CN0409 from Analog Devices and the SEN0189 from DFRobot. The two sensors are designed for different applications; the CN0409 is designed to give exact measurements on liquids in a test tube, while the SEN0189 is designed to be an inexpensive, easy to use sensor that can be mounted inside an application (such as a dishwasher) and deliver real time measurements.

3.1.1.1 CN0409 in combination with ADICUP360

The CN0409 used in this project is mounted on the sensor card EVAL-CN0409-ARDZ and is used in combination with the EVAL-ADICUP360 open source development board. Both components are from Analog Devices and can be seen in Figure 3.1a. The CN0409 consists of two IR-LED [LED1, LED2] with a wavelength of 860 nm and two photosensors [D1, D2] configured as in Figure 3.1b. This setup makes it possible to implement both nephelometric and attenuation measurements as described in ISO 7027-1:2016 [19]. By combining both sensors located 90° and 180° from the light source, the CN0409 can perform turbidity measurements that closely resemble commercially available turbidity meters, on the interval 0-1000 FTU [23].

The EVAL-CN0409-ARDZ sensor card is, however, not designed for real time measurements since it conducts its measurements on samples in a test vial. The CN0409 was used to explore how much the combination of a 90° and 180° sensor improves the measurement.

(a) Photo of CN0409 connected to ADICUP360

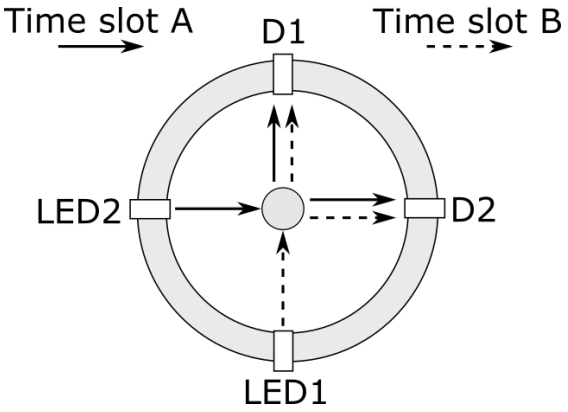

(b) CN0409 consists of two LED [LED1, LED2] and two photo detectors [D1, D2].

Figure 3.1: The first turbidity sensor solution is a CN0409 connected to an ADICUP360

The CN0409 operates in two time slots, SlotA and SlotB as shown in Figures 3.1b and 3.2. During SlotA, LED2 is emitting light and during SlotB LED1. During the active period, both D1 and D2 collect data. The measurements collected between SlotA and SlotB are used to remove the effect of ambient light from measurements in SlotA and SlotB. The number of LED pulses during each time slot can be varied between 1 and 128 pulses, an average is then calculated and sent to the development board. When the measurement data become available in the development board it is possible to extract it using a terminal and a UART connection.

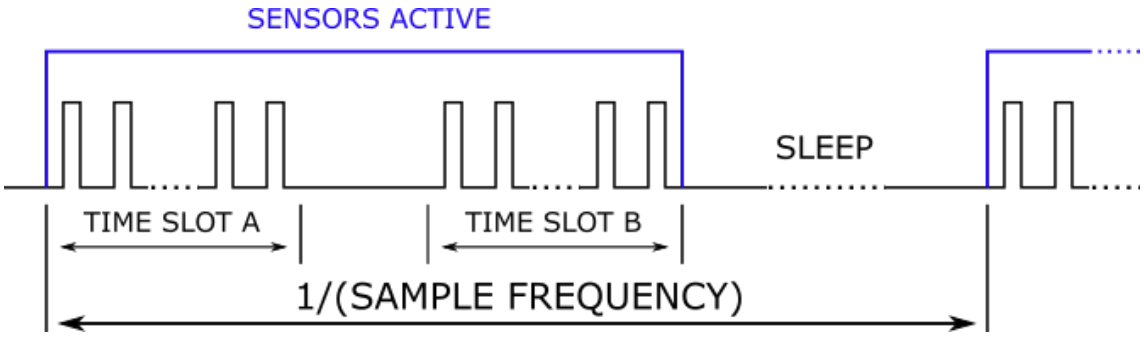

Figure 3.2: Timing diagram for CN0409.

3.1.1.2 SEN0189 in combination with Arduino UNO

The turbidity probe SEN0189 from DFRobot outputs a voltage that is proportional to the received light by the photodiode. The SEN0189 is connected to an Arduino UNO and has a resolution of 4.9 mV. The maximum voltage (4.5 V) corresponds to that no light is absorbed by the liquid and 0 V corresponds to that all light is absorbed. The probe can be mounted inside an application and is thus suited for real time measurements of both still and flowing liquids. The Arduino UNO takes 100 μs to read an analog input, giving it a maximum sample rate of 10 000 Hz [24]. In the specification for the SEN0189, the response time is faster than 500 ms [17] giving it a sample rate above 2 Hz. During the tests the SEN0189 delivered realistic results for sample frequencies up to 100 Hz. This sensor setup can be seen in Figure 3.3.

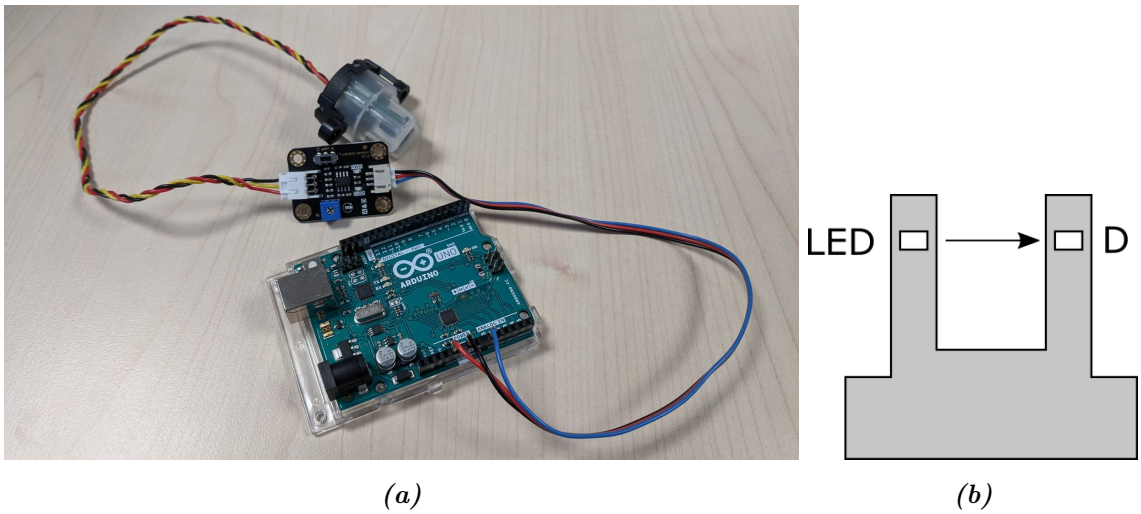

Figure 3.3: ***(a)*** Photo of SEN0189 with Arduino UNO. ***(b)*** Simple schematic showing positions of the LED and photodiode (D) in SEN0189.

3.1.2 Ultrasonic sensors

As described in Section 1.2.2 most of the literature uses transducers with a center frequency between 2 and 3 MHz. There are also two dominating hardware setups for measuring particle concentration. The first one uses one transducer in combination with a pulser/receiver. The second one uses two transducers, an oscilloscope and a function generator. Since an oscilloscope and function generator is available the second hardware setup will be used.

Finding an ultrasonic transducer with a reasonable delivery time proved to be a challenge. Most of the commercially available transducers are designed for a specific application, such as distance measuring, which outputs a voltage corresponding to the distance between the sensor and the measured object. To use the techniques described in the literature one needs to measure the raw voltage created by the transducer's piezoelectric element. Another problem is that most ultrasonic transducers have a center frequency in the kHz range and not MHz.

In this study one ultrasonic transducer will be tested, the UB162M4 from PUI Audio Inc (see Figure 3.4a). The UB162M4 has a center frequency of 2.45 ±0.1 MHz and is rated for a voltage of 100 V peak to peak. In the testing of the ultrasonic sensors, the signal was generated using the function generator HM8150 from RHONDE&SCHWARTZ capable of outputting high frequency signals. The signals were sampled using a Tektroniks MSO2014 oscilloscope and the captured waveforms exported to a computer.

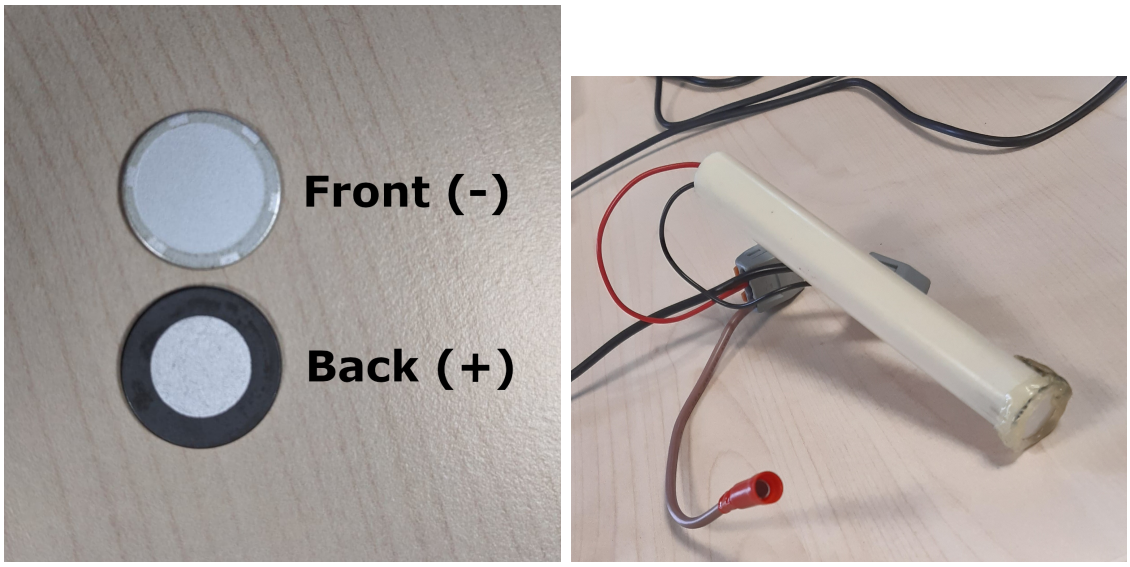

(a) *(b)*

Figure 3.4: ***(a)*** The ultrasonic transducers UB162M4 from PUI Audio Inc. ***(b)*** UB162M4 prepared for use in test rig.

3.2 Test rigs

Two test rigs were built, one for tests in still water and one for flowing water. The purpose of the still water test rig is to have a controlled environment to test the sensors. An illustration of the still water test rig can be seen in Figure 3.5a. It consists of a 1.5 l container with slots for inserting the ultrasonic sensors.

The purpose of the test rig for flowing water is to observe if and how the sensors' performance differs from the still water case. The flowing water test rig is constructed mainly by three parts connected with tubing. An illustration of this can be seen in Figure 3.5. The three parts are a container, a pump and a sensor box. The container was used in order to both fill the test rig with water and mix higher concentrations of slurry by adding concrete dust. The role of the sensor box was to provide a container where sensors could be placed, and the flow of slurry through it could be controlled. The sensor box contained turbidity probe, ultrasonic sensor and a pressure sensor. On the outlet of the sensor box, a flow sensor was placed. In order to prevent sedimentation forming on the bottom of the sensor box, the sensor

box was placed vertically.

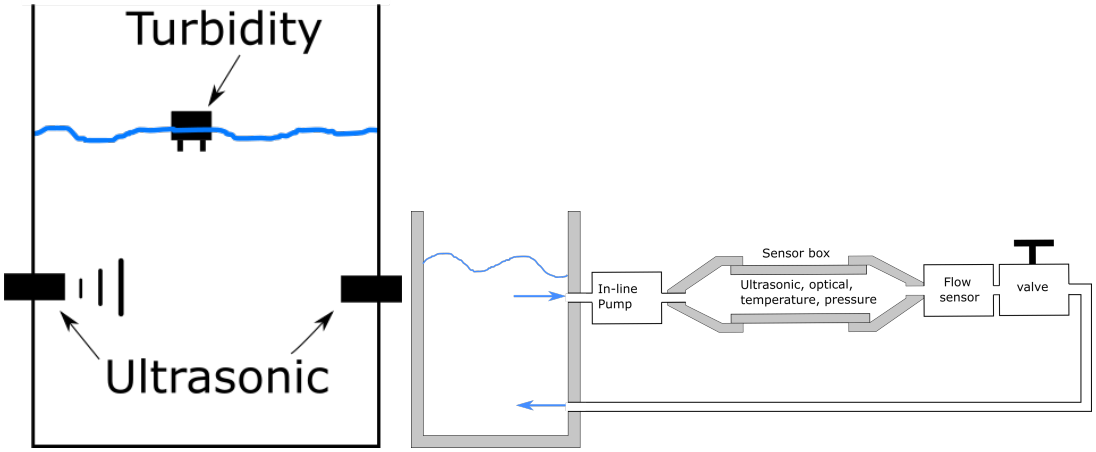

(a) Test rig still water *(b)* Test rig flowing water

Figure 3.5: Illustration of the two test rigs

4

Tests

In this chapter, the different tests conducted using the sensors will be presented. For each test, a description of how the test was conducted is given followed by the results of that test. Discussions regarding the results will also be presented in conjunction with each test.

4.1 Visual comparison of different concrete slurry concentrations

In order to get an intuitive understanding of how concrete slurry looks and behaves for different concentrations, a visual comparison was conducted. A large batch of concrete slurry was mixed by adding concrete dust to water in order to reach a specific volume concentration. Photos of the different concentrations can be seen in Figure 4.1. One thing to note is that no visual difference could be seen for samples above 0.5%. By comparing these samples with recycled slurry water gathered in informal testing, using an existing water management system that is out on the market. It was concluded that the estimated slurry concentration after a slurry recycling machine would probably be below 2%. The recycled slurry water that was used in the comparison can be found in Appendix A.2.

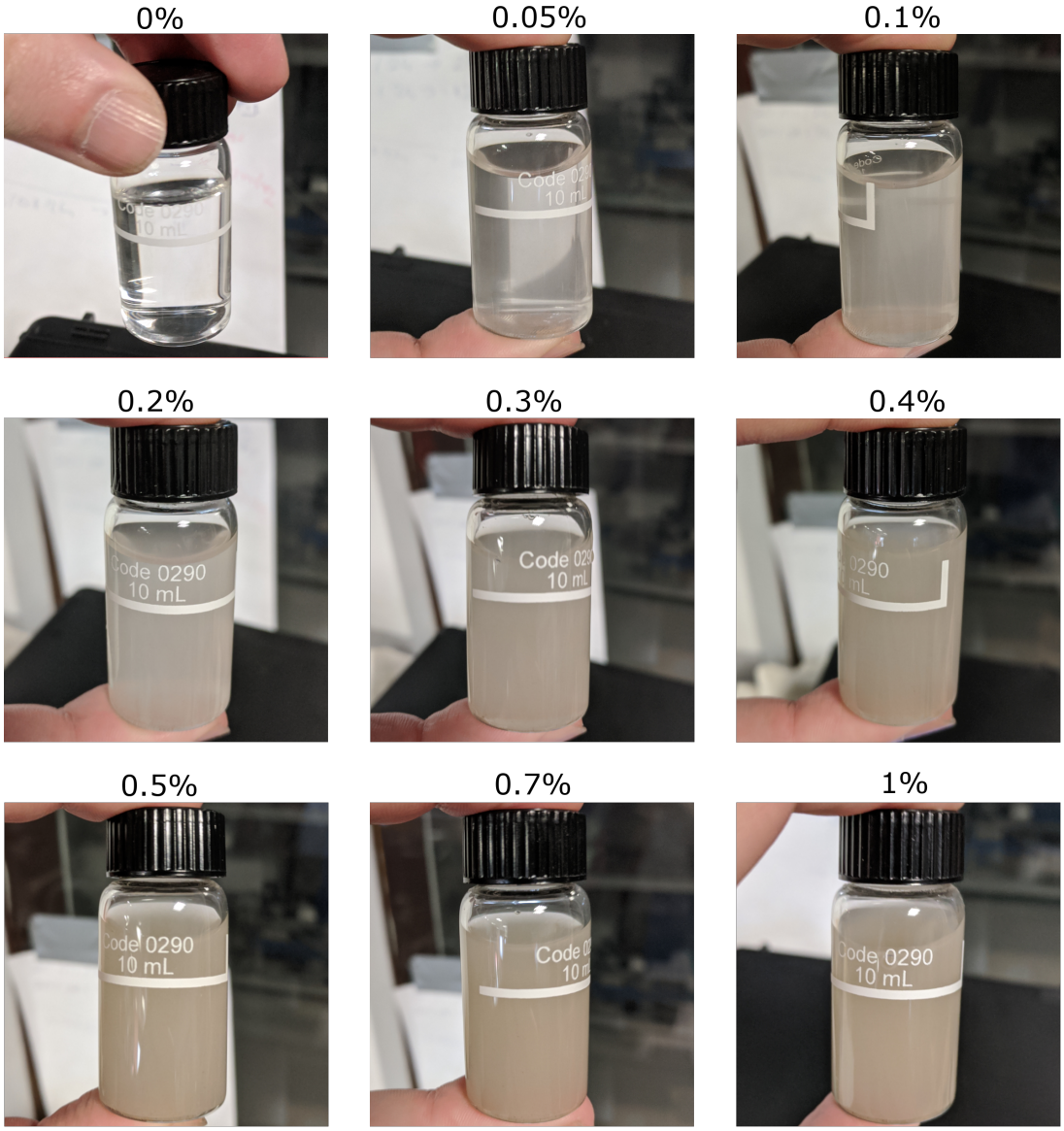

Figure 4.1: Samples of concrete slurry with concentrations ranging from 0% to 1%.

4.2 Testing of ultrasonic sensors

The ultrasonic sensors were tested on different concentrations and with different distances between the sensors in order to compare and analyze their behavior. The function generator connected to the ultrasonic transmitter was set to produce a constant sine wave with a frequency of 2.47 MHz. The frequency 2.47 MHz was chosen since this frequency generated the strongest signal in both the transmitter and the receiver. The oscilloscope was set to measure both the transmitted signal (V_0) and the received signal (V_r). These signals were then imported to a computer where they were saved and compared.

4.2.1 High concentration and distance testing

In order to find out at what distance the sensors should be placed from each other, three different distances were tested: 15, 30 and 60 mm. Measurements were taken on a range of eleven concentrations of slurry, using the still water test rig. In order to establish a operating range for the sensor, a guess based on [11] was made of what might constitute high concentration slurry. As a starting point, measurements were taken on 0% slurry up to 10%, in 1% increments. On each concentration, two measurement samples were taken. Tests were repeated at a different time to test the repeatability of the results. The slurry was stirred by hand in between measurements, in order to keep the slurry from sedimenting.

Since Equation (2.4) can be rewritten as $V_r/V_0 = e^{-\alpha d}$, where α is linearly dependent on the concentration, the strength of the signal is expected to decrease exponentially as the concentration of the slurry increases. The measurements were evaluated by examining and comparing the maximum value of the Fourier transform of each measured signal and concentration. By doing so all low frequency disturbances, compared to the 2.47 MHz signal, were filtered out. The result from these measurements can be seen in Figure 4.2.

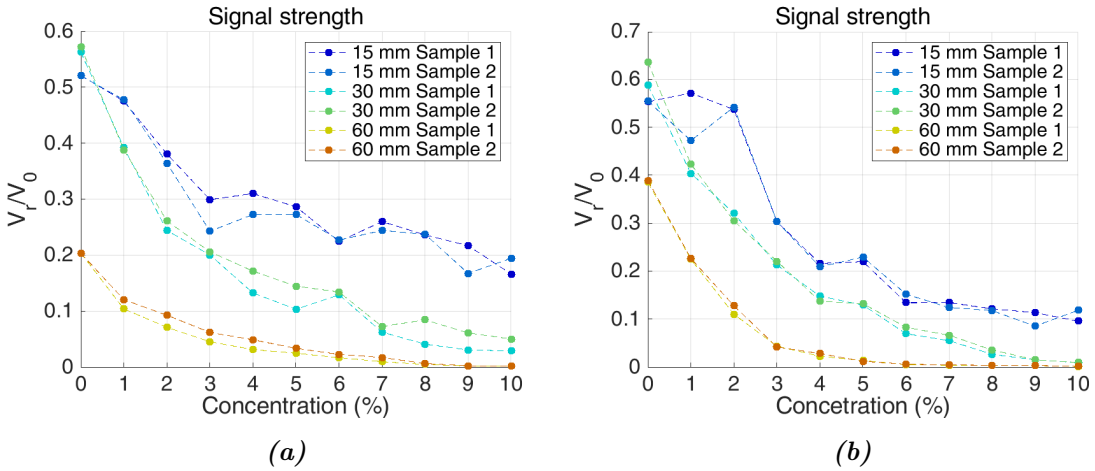

Figure 4.2: Results of measurements on concrete slurry ranging from 0% to 10% using the ultrasonic sensor. The transducers were placed with a distance of 15, 30 and 60 mm between them. ***(a)*** Test number one and ***(b)*** Test number two.

It can be observed that the ratio between V_r and V_0 for the 0% measurement differs in Figures 4.2a and 4.2b. This is because the ultrasonic transducers are very sensitive to how they are placed related to each other. A small difference in the angle between the transmitter and the receiver resulted in a large difference in amplitude.

As described in [9], the natural logarithm of V_r/V_0 should be linearly dependant on the concentration. The natural logarithm of V_r/V_0 can be seen in Figure 4.3 and it can be concluded that a linear model with additive noise could be a good model for this signal. It can also be observed that the signal to noise ratio is highest for the 60 mm setup and lowest for the 15 mm setup. One theory for this is that more

particles pass between the sensors when a greater distance is used, thus resulting in a greater energy loss per concentration. Since the energy loss is correlated to the concentration, a greater energy loss gives a better signal resolution and a higher signal to noise ratio.

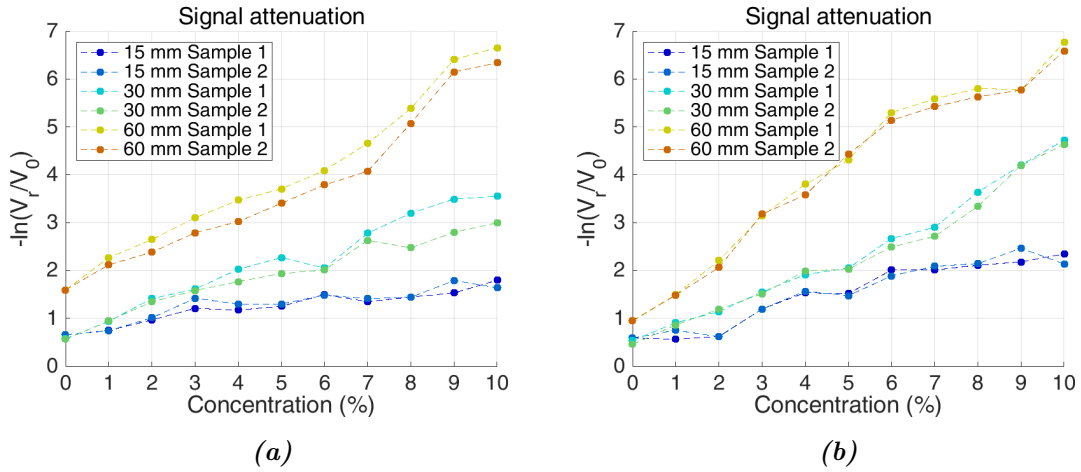

(a) *(b)*

Figure 4.3: Attenuation of the transmitted signal through increasing levels of concentration of slurry. ***(a)*** Test number one and ***(b)*** test number two.

4.2.2 Low concentration testing

From the high concentration testing, it was concluded that the signal to noise ratio was too low when the distance between the transducers was 15 mm. Thus this distance between the sensors was omitted for the testing on lower concentrations. The test was conducted by measuring concentrations between 0% and 2% with 0.4% increments. The distance between the sensors was 30 mm and 60 mm and all measurements were made in the still water test rig.

Another change that was introduced was the inclusion of a water pump to circulate the slurry in the container. The previous method of stirring the slurry still allowed for some sedimentation to occur and was deemed to be a larger problem in the measurements than the disturbances introduced by the pump.

The data from these tests were analyzed in the same way as the previous, by examining and comparing the maximum value of the Fourier transform of each measured signal and concentration. The results from these tests can be seen in Figures 4.4 and 4.5.

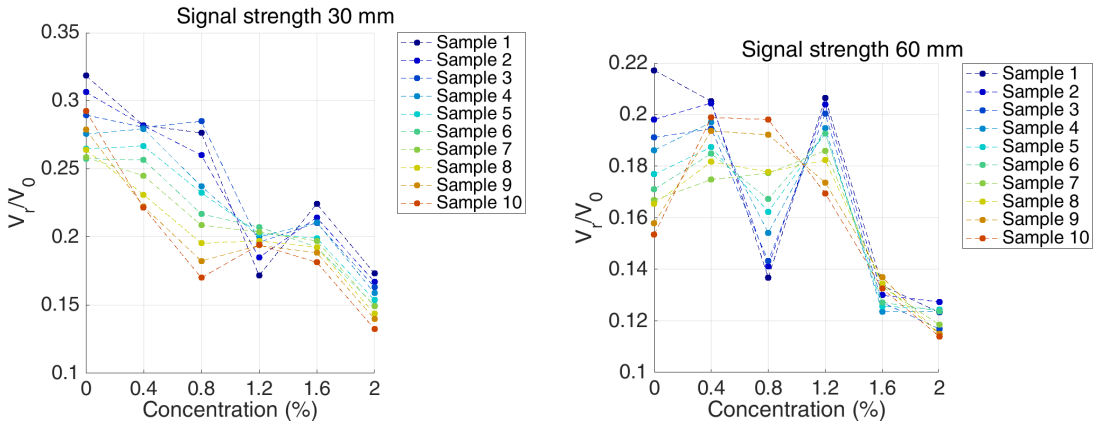

(a) *(b)*

Figure 4.4: Results of measurements on concrete slurry ranging from 0% to 2% using ultrasonic sensors. ***(a)*** Test number one and ***(b)*** test number two.

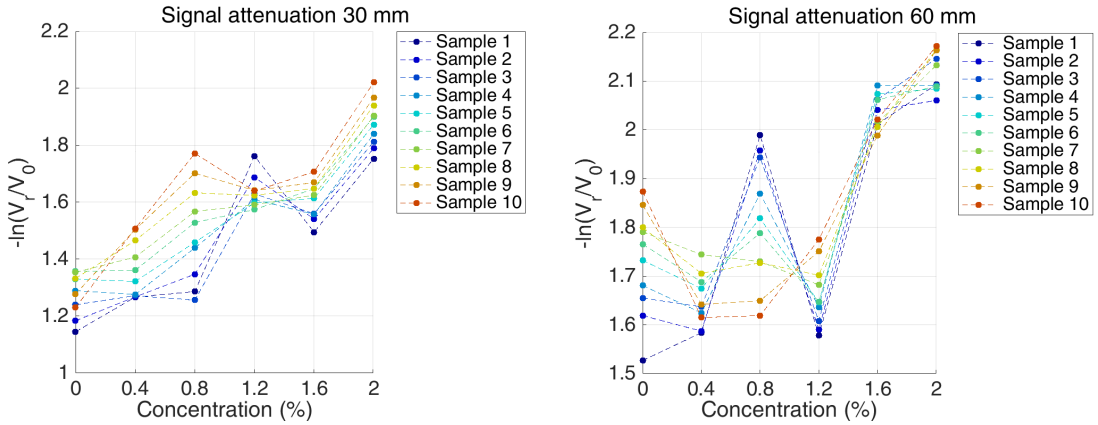

(a) *(b)*

Figure 4.5: Attenuation of the measured signal on low concentration concrete slurry. ***(a)*** Test number one and ***(b)*** test number two

It can be observed that the signal to noise ratio is lower in this test on low concentrations than the test on high concentrations. One reason for this can be that more samples are taken on each concentration and thus give a better visualization of the true noise. Another reason can be that the performance of the ultrasonic measuring technique experience large noise when measuring on low concentrations.

An interesting observation is that for the samples for concentration 1.6% and 2% in Figures 4.4a and 4.5a is ordered after the sample number. This is also true for the measurements on clear water (0%) in Figures 4.4b and 4.5b. The samples are taken with a short time between them, so this ordering indicates a drift over time and not white noise. This drift seems to be the major disturbance in these measurements.

4.2.3 Temperature testing

The drift observed in the low concentration tests in Section 4.2.2 indicates a change in the attenuation parameter α in Equation (2.4). Since this parameter encompasses many different factors that could change over time, it is difficult to know exactly what causes this drift. The factor that was deemed the most probable to cause this drift was temperature, since both [10] and [25] list temperature being one of the factors that affects the attenuation parameter. Since cold tap water with an approximate temperature of 16°C was used during the experiments, the temperature would rise towards the room temperature of approximately 19°C.

To test the correlation between the change in temperature and the drift, three tests were performed. In two of them, cold tap water was used. The water was first sampled, then heated using a heat gun and then sampled again. This process was then repeated until the test was finished. In the third test, the tap water was placed at room temperature overnight. The water was then sampled, a time period of about 10 min passed and the water was sampled again. This process was then repeated until the test was finished. All of these tests were performed on the still water test rig and can be seen in Figures 4.6 to 4.8.

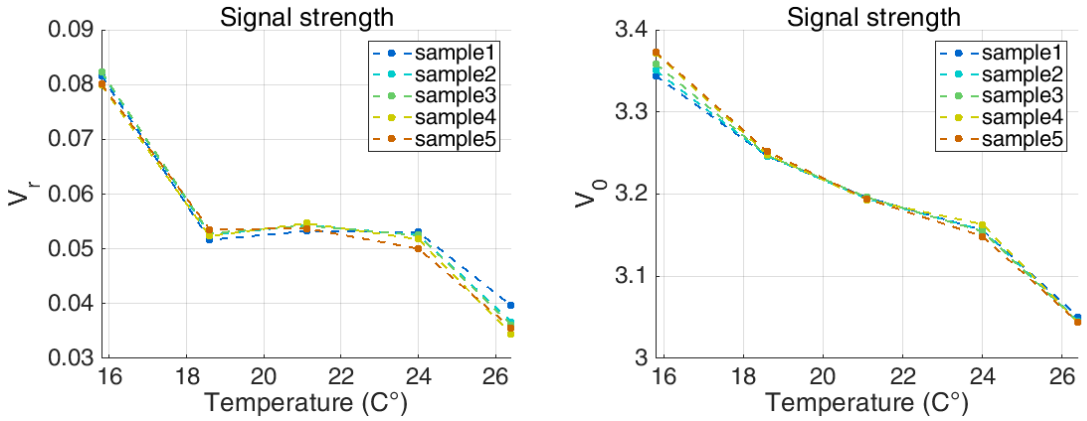

(a) *(b)*

Figure 4.6: The first ultrasonic test on different temperatures. During this test, the transducers were placed at a distance of 60 mm between them. The graph in ***(a)*** shows the voltage over the receiver and ***(b)*** shows the voltage over the transmitter.

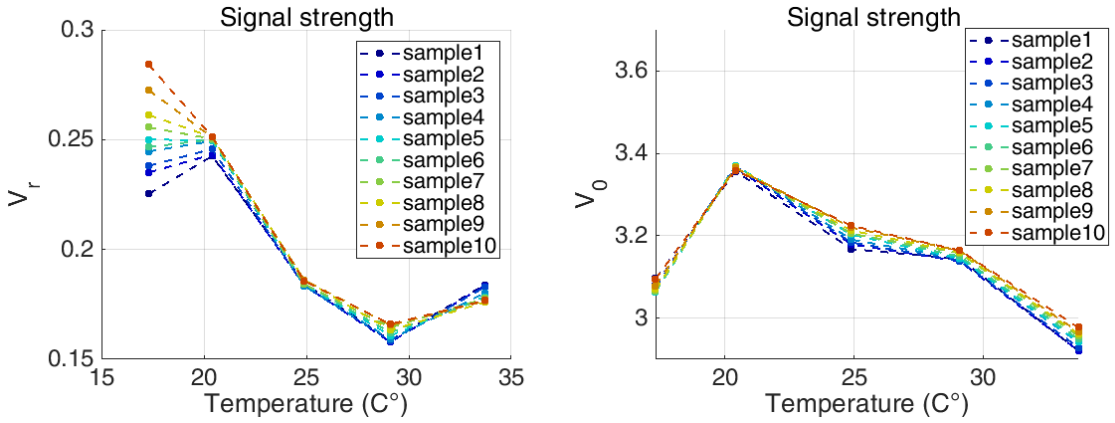

(a) *(b)*

Figure 4.7: The second ultrasonic test on different temperatures. During this test, the transducers were placed at a distance of 60 mm between them. The graph in ***(a)*** shows the voltage over the receiver and ***(b)*** shows the voltage over the transmitter.

In Figure 4.6 the transmitted signal (V_0) seams to decrease with temperature. A decreasing pattern can also be seen in the received signal (V_r), this can however be correlated to the decrease in the transmitted signal and not to changes in the attenuation coefficient α. In Figure 4.7 the drift does not have a clear correlation with temperature.

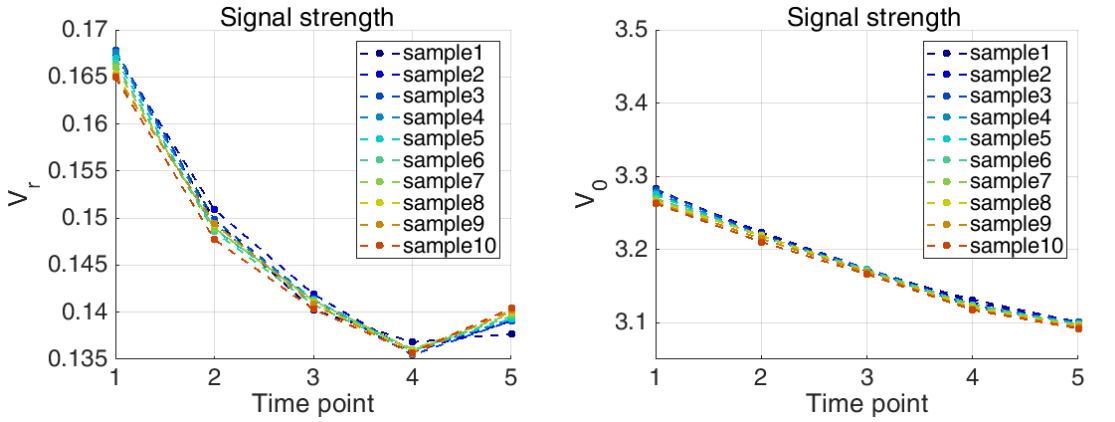

(a) *(b)*

Figure 4.8: Measurement of drift over time using the ultrasonic transducers. Samples where taken at different points in time. Between each time point approximately 15 min passed and at each time point 10 samples are taken with approximately 10s between them. During this test, the transducers were placed at a distance of 60 mm between them. The graph in ***(a)*** shows the voltage over the receiver and ***(b)*** shows the voltage over the transmitter.

In Figure 4.8 a drift can be observed for both V_r and V_0. This test, with constant temperature, seems to follow the general trend of decreasing signal strength with

time, which is also seen in the temperature tests.

By comparing the results with a temperature change in Figures 4.6 and 4.7, with the result of the test where the temperature was kept constant in Figure 4.8. It can be concluded that the drift cannot be attributed to solely a change in temperature. Another likely theory is that the function generator used to create the 2.47 MHz sine wave was not able to keep a steady output for the high frequency signal. More figures showing the variation of V_0 during tests can be seen in Appendix A.1. For a better investigation of what might have caused the drift, another function generator would have to be tested but that was not possible within the scope of this project.

4.2.4 Test on flowing slurry

Two tests were performed to examine how this ultrasonic measuring technique works on flowing slurry. During these tests, the transducers were placed with a distance of 16 mm between them and the slurry was flowing with an approximate velocity of 0.62 m/s, based on the readings from the flow meter and the dimensions of the sensor box. The short distance between the sensors was chosen in order to get a higher flow of the slurry through the sensor box. Tests were performed on concentrations from 0 to 2% with 0.2% increments and the results can be seen in Figure 4.9.

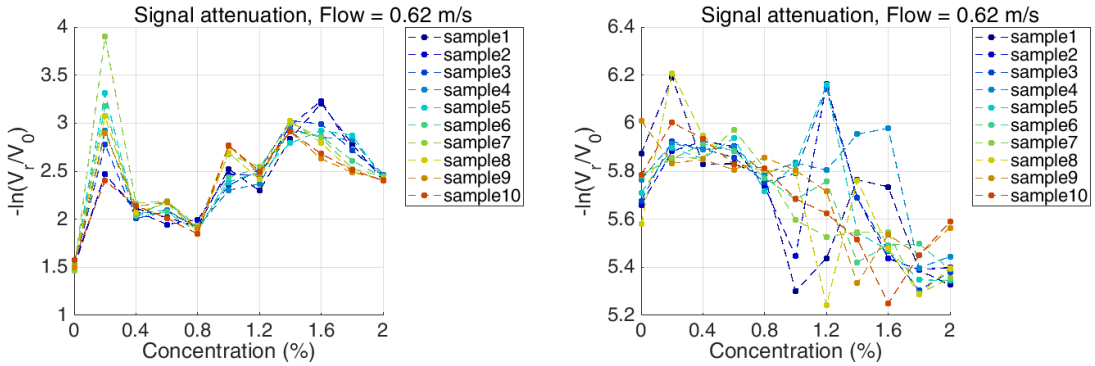

(a) *(b)*

Figure 4.9: Ultrasonic attenuation measurements performed in flowing water. The measurements in ***(a)*** and ***(b)*** were conducted under the same conditions.

The results from the tests on flowing slurry do not fit the linear model presented in Equation (2.5). Small bubbles formed on the surfaces of the sensor box during the tests. One of the surfaces that they formed on was the transducers. This introduced both noise and a bias correlated to the number of bubbles on the transducers. In order to try and remove the bubbles, the flow of the water was increased and the sensor box was shaken. This did not remove the bubbles so the testing had to continue with the bubbles. In Figure 4.10 an image of the problem can be seen. Note that most of the bubbles are stuck on the walls and transducers, not free in the water column.

Figure 4.10: Image showing the bubbles on the surfaces of the sensor box and the transducer.

4.3 Testing of SEN0189 turbidity probe

The turbidity probe was tested for its performance for different ranges of concentrations. For high and low concentration testing, measurements were taken with and without a pump to circulate the slurry. Measurements were first taken on the slurry with the pump running, in order to avoid sedimentation. Then with the pump turned off, so that measurements were taken during the sedimentation process. Since Equation (2.2) can be rewritten as $I = I_0 e^{-\sigma d c_n}$, the loss of signal strength is expected to decrease exponentially as the concentration of the slurry increases.

4.3.1 High concentration testing

In order to explore the upper limit of the SEN0189 turbidity probe, measurements were performed on slurry concentrations from 0% to 7% in 1% increments. Because of the exponential decrease of signal strength as the concentration increases, at some point the measured light intensity will become lower than the sensor noise, and this will decide the operating range of the sensor.

In Figure 4.11 the results from the high concentration test, with and without pump, can be seen. In Figure 4.11a the rate at which sedimentation occurs can be seen. As the dust settles, more light penetrates the medium, and a higher voltage is generated by the photodiode. By comparing Figures 4.11a and 4.11b it can be concluded that using the pump while preventing sedimentation, is adding some additional noise to the measurements.

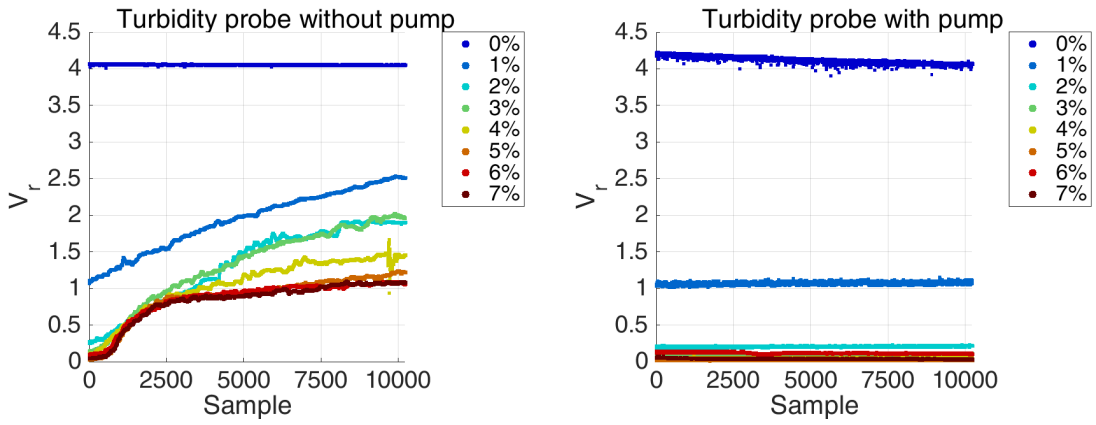

Figure 4.11: Measurements using the SEN0189 turbidity probe, ***(a)*** without a pump circulating the slurry and ***(b)*** with a pump circulating the slurry.

As seen in Figure 4.12, the concentration at which the turbidity probe becomes unable to detect any of the transmitted light can be observed. For any of the measurements on concentrations larger than 2%, there is not enough light transmitted from the LED to the photodiode in order to distinguish between the concentrations.

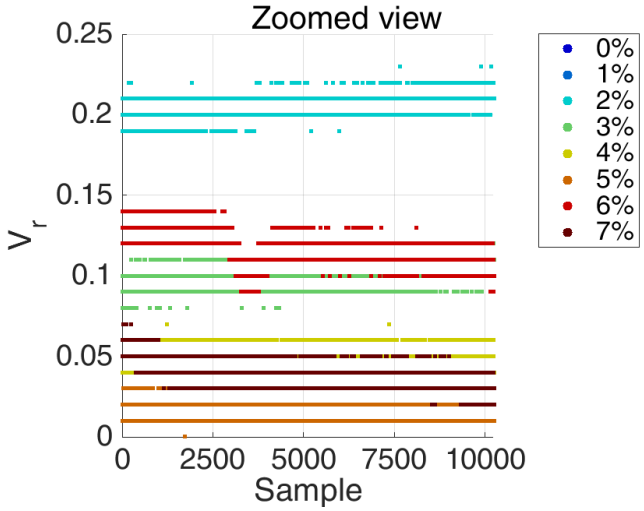

Figure 4.12: Zoomed view of the higher percentages of Figure 4.11b, showing how it is not possible to distinguish between the measured concentrations because of the low signal to noise ratio.

4.3.2 Low concentration testing

After deciding the operating range of the sensor probe, its performance was tested on lower concentrations of slurry. This resulted in two more tests; one on 0-1% and one on 0-2% concentration of slurry.

From the results of the low concentration testing on concentrations from 0% to 2%, seen in Figure 4.13, the exponential decrease between the concentrations can be seen. The large disturbance in the measurements of slurry at a 2% concentration seen in Figure 4.13b was due to an outside disturbance not related to the test.

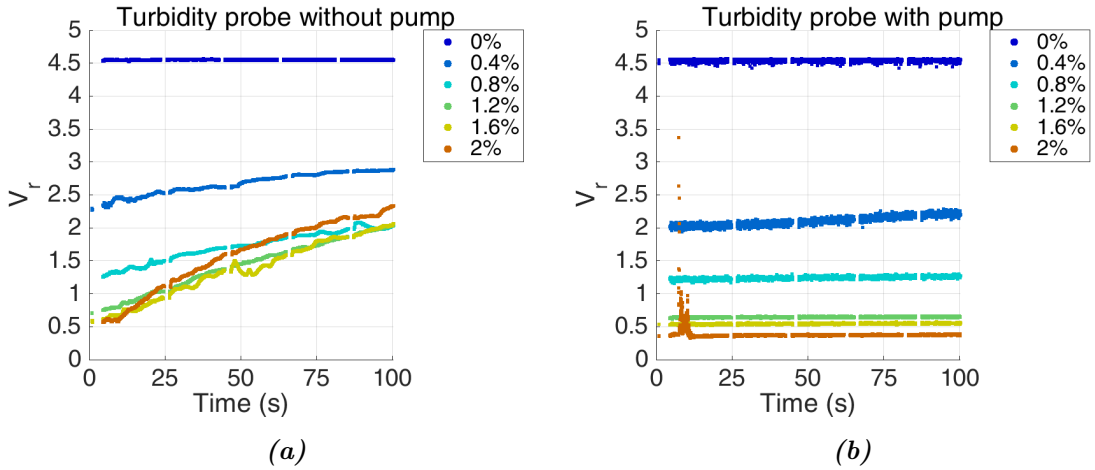

Figure 4.13: Measurements using the SEN0189 turbidity probe, ***(a)*** without a pump circulating the slurry and ***(b)*** with a pump circulating the slurry.

The results from low concentration testing of the turbidity probe on concentrations ranging from 0% to 1% can be seen in Figure 4.14. In the measurements with a pump to circulate the water seen in Figure 4.14b, a great deal of measurement noise can be observed for two different concentrations. In order to get a more clear result, a moving average filter with a length of 100 samples was applied to the measurement data from this test.

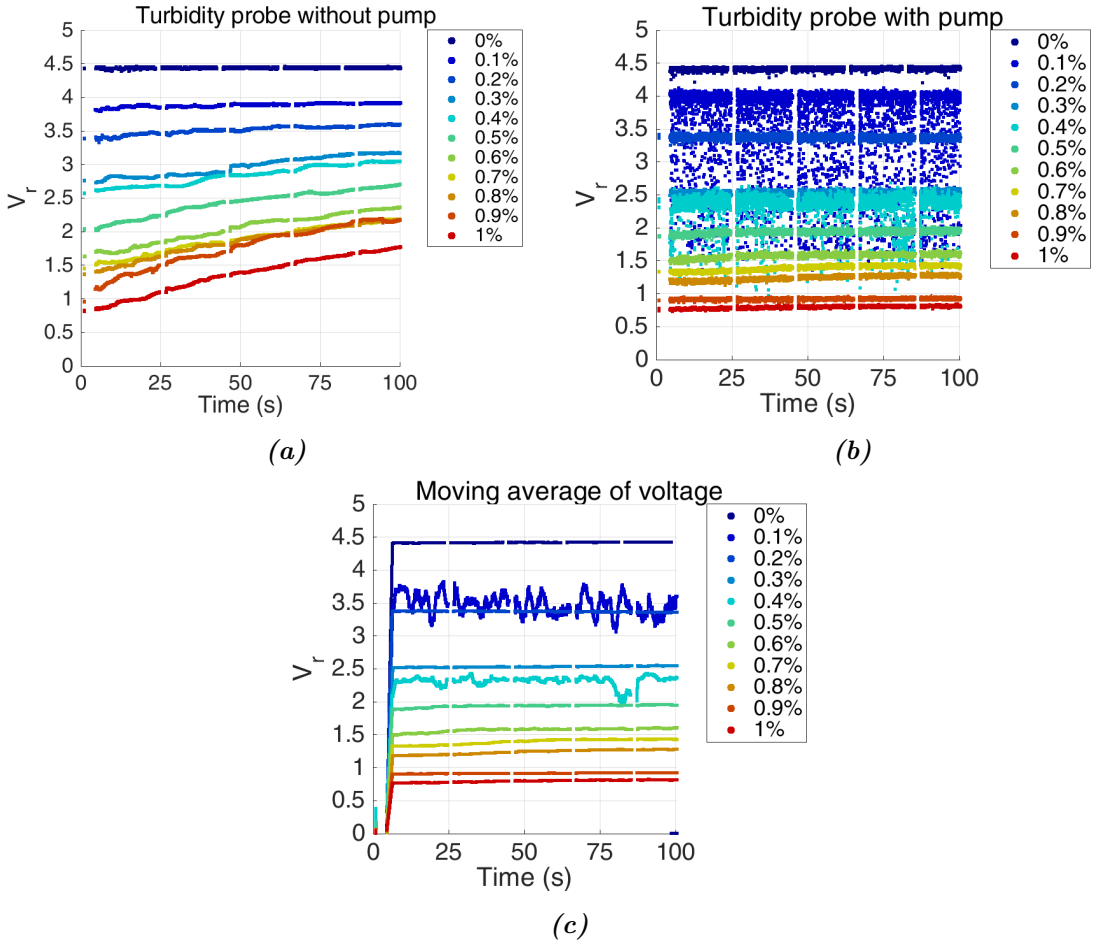

Figure 4.14: Measurements using the SEN0189 turbidity probe, ***(a)*** without a pump circulating the slurry and ***(b)*** with a pump circulating the slurry. In ***(c)*** a moving average filter has been applied to the measurement displayed in ***(b)***.

The large amount of measurement noise that can be observed in the results from the measurements on the range of 0-1%, seen in Figure 4.14b, can be attributed to the pump creating a bubbling surface of the slurry. Depending on the placement of the pump and the direction of the pump outlet compared to the inlet of the pump, different flows in the container could be created. Having the pump arranged in a way that left room for the turbidity probe, meant that the pump needed to be placed in such a way that created some upward flow and disturbed the surface of the slurry in the container. Since the turbidity probe measures from the surface and the flow from the pump causes bubbles on the surface, at times causing the level of the slurry to dip below the sensor, some disturbances were introduced. Even if the pump made it difficult to take good measurements on the slurry, it was necessary in order to measure overtime on a sample and not be affected by the sedimentation.

The mean of the received voltage from the two low concentration tests (seen in Figures 4.13b and 4.14b) was calculated. Plotting the mean of the voltage against the concentration measured indicates, that the voltage decrease exponential with respect to the concentration. This is shown in Figure 4.15 for both low concentration

tests.

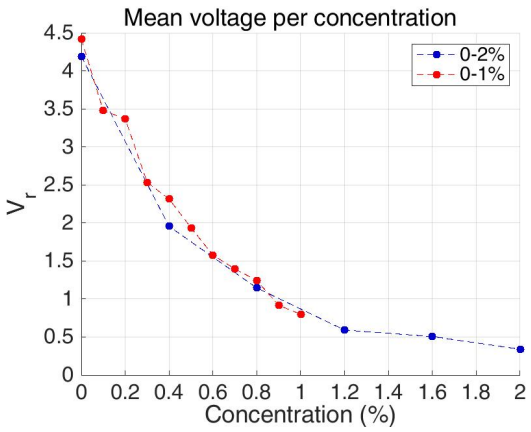

Figure 4.15: Graph displaying the mean voltage from the measurements presented in Figures 4.13b and 4.14b. This figure indicates that the measurements decrease exponentially with concentration.

The linear relationship between the attenuating light intensity and the concentration can be seen in Figure 4.16. In Figure 4.16a all data points from both low concentration tests are used to create a linear regression model by fitting a line to the data points using a MMSE estimator. By comparing Figure 4.1 and the results from the measurements on filtrated slurry water in Section 4.5, the concentration from the recycled slurry water can be estimated to be in the range between 0.2-0.4%. From Figure 4.16a it can be deduced that by modifying the data set by removing the two last data points (corresponding to the measurements at 1.6% and 2%) the line can be better fitted to the lower, more relevant concentrations. This model from the modified data set can be seen in Figure 4.16b.

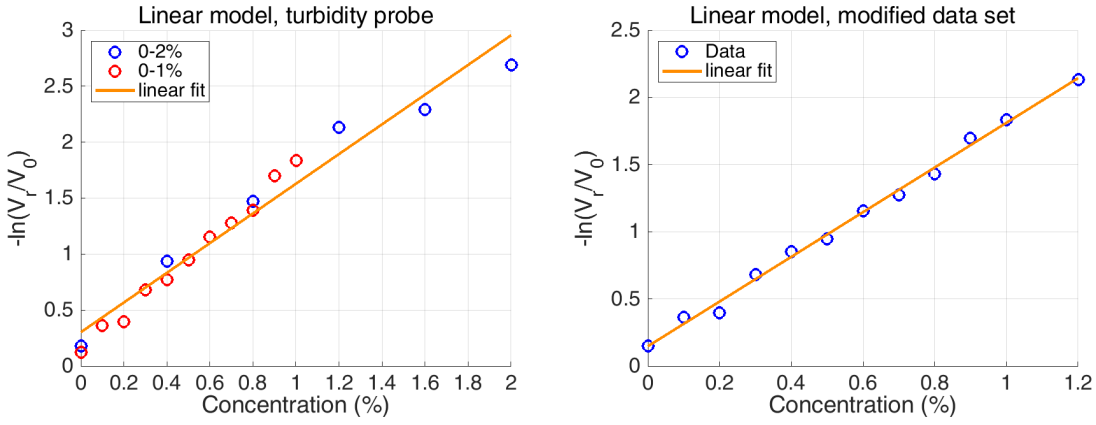

(a) ***(b)***

Figure 4.16: Linear models for mapping between the attenuation and concentration for ***(a)*** complete data set and ***(b)*** modified data set, where the two last measurements have been removed.

4.3.3 Test on flowing slurry

In order to test the performance of the SEN0189 turbidity probe on flowing slurry, two different tests were conducted. The purpose and the setup of the two tests were identical and used in order to get a larger sample size. For both tests, measurements were done on a range of low concentrations of 0% to approximately 2%. As for the testing of the ultrasonic sensors, the slurry had an approximate flow rate of 0.62 m/s.

In Figure 4.17 the results from measurements with the turbidity probe in the flowing water test rig can be seen. Compared to the measurements taken on the still water test rig, the measured received voltage at each concentration is substantially lower. The measurements on the flowing water test rig also contain more measurement noise. Less measurement noise can be observed as the concentration of the slurry increases. A moving average filter of length 100 samples was used in order to compensate for the added noise levels.

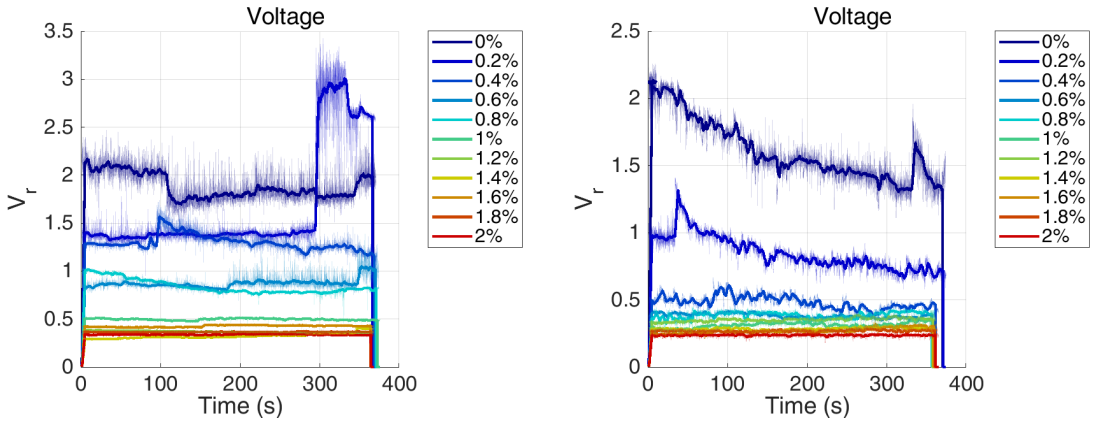

Figure 4.17: Moving average filter and raw data of measured voltage from turbidity probe in flowing water test rig sensor box. Figure ***(a)*** and ***(b)*** displays the same test preformed at two different times.

In Figure 4.18, the average voltage measurements per concentration form Figure 4.17, and a line fitted to the attenuation data from the two different tests can be seen.

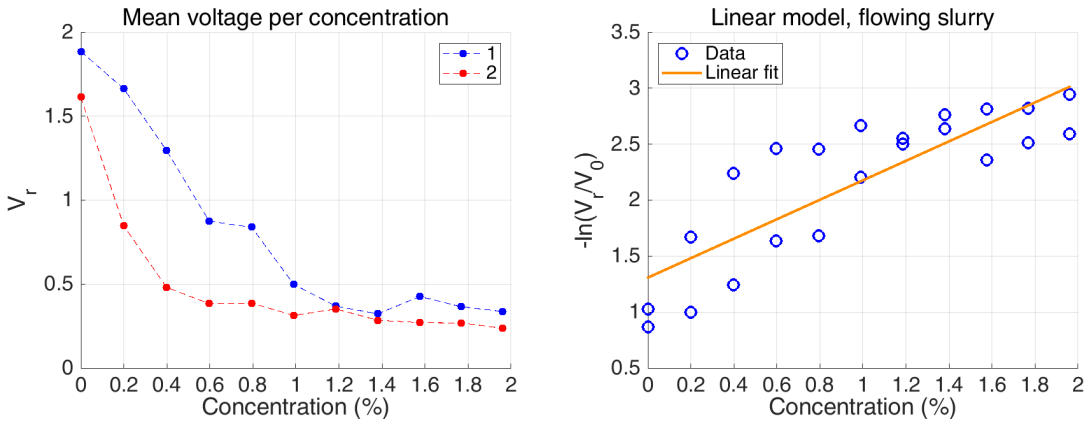

(a) *(b)*

Figure 4.18: ***(a)*** Average measured voltage per concentration where 1 and 2 is calculated from the data in Figure 4.17a and Figure 4.17b. ***(b)*** A linear regression model of the attenuation of the data in ***(a)***.

Comparing the results from the low concentration testing with the results from the testing on flowing water/slurry, some interesting differences can be found. One large, and important difference is the level of the voltage generated by the photodiode. From both tests conducted on the flowing water/slurry test rig, the generated voltage for clean water was around 2 V. The generated voltage in the still water/slurry test rig was around 4.5 V for clean water. Another more noticeable one is the increased noise that is found in the measurements taken on the flowing slurry. Some of the noise is easily handled by a moving average filer, as can be seen in Figure 4.17, but some source of disturbances causes an occasional large jump in the received voltage. Deciding the definitive reason behind these disturbances would require more testing but there are some probable factors that were observed during the testing. The most obvious one is the factor that was the purpose of the testing on the flowing water test rig i.e., the flow.

Figure 4.19: Image showing the air bubbles on the surfaces of the sensor box and the turbidity probe.

If no other factors were observed then a drop in generated voltage and increased levels of disturbances would safely be assigned to the flow, but during the testing,

a large number of air bubbles filled the sides of the sensor box, both in front of the LED and the photodiode. Having a layer of air in front of either one of them would increase the breaking index compared to water since it is less dense and would cause more light to be reflected. Another factor that could play a part in these disturbances is a thin layer of dust that remains on all surfaces after they have been in contact with concrete slurry. This thin layer of very small particles gets stuck in the microstructure of the equipment and does not get washed away with water. Speculating on the reasons for the disturbances lead to the presumption that the air bubbles are responsible for a large decrease in the generated voltage, and if some of them would move, and leave the LED and photodiode clear from air bubbles, a large spike in the received voltage would be registered, as can be seen in Figure 4.17a. The flow is probably responsible for the increased measurement noise and the thin layer of dust lowers the amount of light that gets through, thus decreasing the generated voltage.

The effects of the noise and disturbances that are present in the measurements on the flowing water test rig but not on the still water test rig can clearly be seen when comparing the linear regression models of the light attenuation seen in Figures 4.16 and 4.18b.

4.4 Tests preformed using the sensor card CN0409

The main goal of the tests performed on the CN0409 is to give a practical understanding of the NTU/FNU/FNRU units. Tests are also made to see if the two measurement angles used in the CN0409 can give a better estimation of the particle concentration.

4.4.1 Measurement of calibration fluids

This test was performed using calibration fluids of 0.02, 10, 100, 1000 NTU. The aim of the test was to give a visual understanding of different turbidity values, give a baseline measurement as well as give an indication of the sensor's sensitivity and noise level.

In Figure 4.20 the calibration fluids for 0.02, 10, 100, 1000 NTU can be seen. It can be observed that the difference between 0.02 and 10 NTU is hard to spot with the naked eye, even though it is possible. It can also be observed that solutions below 100 NTU are really clear in the context of recycled slurry water.

Note that the calibration fluids are formazine suspensions. Thus 0.02 NTU corresponds to 0.02 FNU/FNRU/FAU, 10 NTU corresponds to 10 FNU/FNRU/FAU, and so on.

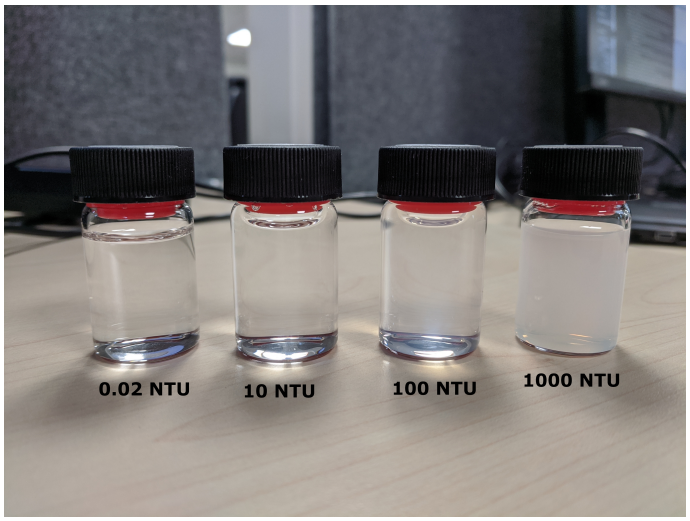

Figure 4.20: This figure shows the calibration fluids with turbidity values 0.02, 10, 100 and 1000 NTU.

The test results from the measurement on the calibration fluids using the sensor card CN0409 are presented in Figure 4.21. It can be seen that for liquids with turbidity below 100 NTU the sensor at 90° offers a higher resolution than the sensor at 180°. During these tests, the difference between the mean measurement of the 0.02 and 100 NTU solution using the 180° sensor is 7.5 units and has noise with a standard deviation of 1.0 units. If the 90° sensor is used the difference between the means is 354.5 units and has noise with a standard deviation of 1.4 units. This is why the standard ISO 7027-1:2016 [19] recommends only using the 90° measurement on liquids with turbidity below 40 NTU/FNU. The provided code to the sensor card switches between using only the 90° measurement and a ratio between the 180° and 90° measurement at 150 FNU [26]. Observe that when both sensors are used the unit becomes FNRU instead of FNU.

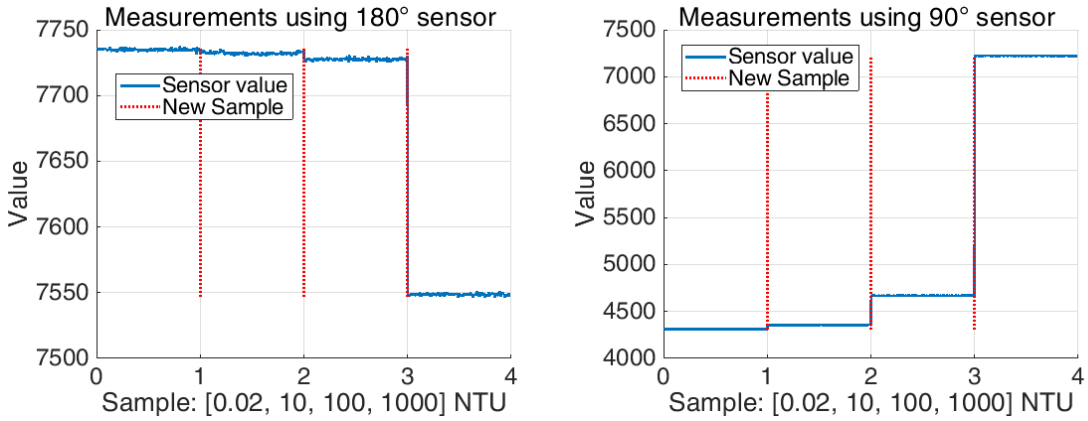

Figure 4.21: This figure shows measurements of calibration fluids with turbidities of 0.02, 10, 100 and 1000 NTU, using CN0409. At each of the red vertical lines, the liquid is changed. For the interval (0,100) NTU there is a small change in the 180° measurement (7.5 units) compared to the 90° measurement (354.5 units)

4.4.2 Measurement of water, tea and coffee

This test was performed using water, tea and coffee. These liquids were chosen since they do not sediment and thus give stable readings. The goal of this test is to show the weaknesses of the turbidity units and why it is important to use the same setup when comparing turbidity measurements with each other.

In both Figures 4.21 and 4.22 the 90° measurement increases when the 180° measurement decreases. It can ,however, be observed that the ratio between the 90° and 180° measurement differs. An example of this can be seen if the measurement of 100 NTU in Figure 4.21 is compared to the measurement of tea in Figure 4.22. The tea have a lower 180° value ($7680 < 7730$) but also a lower 90° value ($4400 < 4700$). The reason for this is that the behavior of light is not only affected by the concentration, some other important parameters are the shape of the particle, particle size and the ability to absorb IR-light.

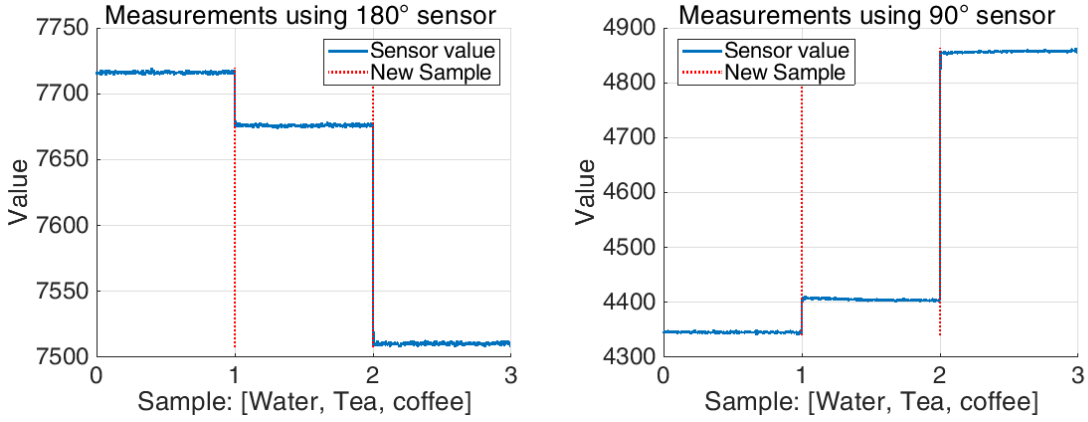

Figure 4.22: This figure shows measurements of water, tea and coffee, using CN0409. At each of the red vertical lines the liquid is changed. It can be observed that the measurement is stable and have a low noise.

As described in Section 2.3.1 the relationship between the 90° and 180° measurement can play an important role when estimating the turbidity level. The estimated turbidity can thus differ a lot depending on the used measurement model. It is therefore important to analyze what equipment and measurement model was that used in order to be able to compare turbidity measurements.

4.4.3 Measurement of unexpected behavior in the CN0409

During tests on low concentrations of slurry (seen in Figure 4.23) the 180° sensor of the CN0409 delivered strange results. According to the theory (see Section 2.3.1) the light passing through the liquid should decrease when the concentration of particles increases, this is also shown using the turbidity probe SEN0189 in Section 4.3. However, the 180° sensors show an increase in light intensity for concentrations between 0.4 and 0.6 percent. The reason for this unexpected behavior is still unclear,

but dose not seem to be limited to the copy of CN0409 used in this project. This behavior has been observed by at least one additional user [27].

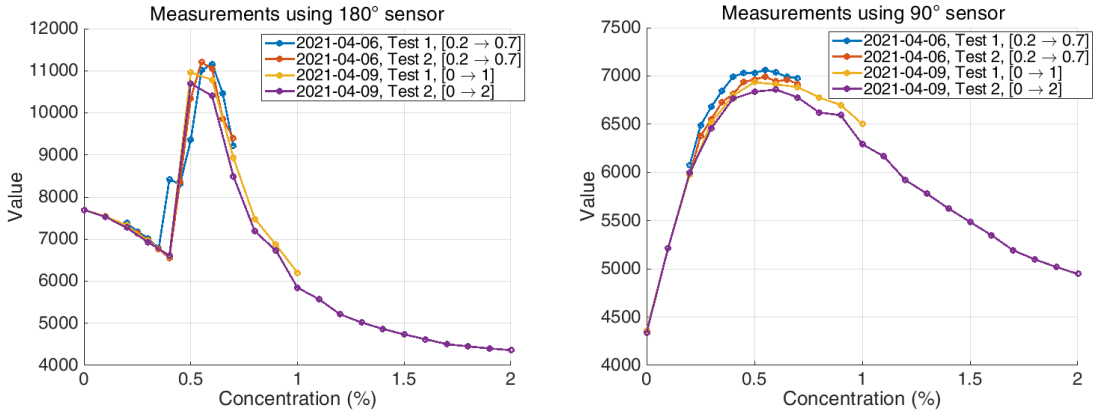

(a) *(b)*

Figure 4.23: This figure shows measurements from slurry concentrations between 0 and 2 % by volume, using CN0409. Each value in the graph is calculated using a mean of the first 4 sensor readings. This is done to minimize the effect of the sedimentation.

4.4.4 Measurement from the sedimentation process

This test was performed to highlight how the sedimentation process affects the possibility to get a good measurement using a test tube. The test also shows how the sedimentation process can be monitored. Observe the measurements in Figure 4.24a and Figure 4.25a is from the same test using the two different sensors.

In Figure 4.24 its possible to observe the sedimentation process using the 180° sensor. At the start of the test (Time = 0) the sensor reading at this time is approximately 4500, which correlates to a concentration around 1.6%. The concentration then decreases and after 70s the sensor reading is around 11000 correlated to a concentration of 0.6%. The sedimentation process continues and it can be observed that the measured value decreases to until Time $\approx$ 130s (Concentration $\approx$ 0.4%), and then increases until the end of the test (Concentration $\approx$ 0.3%).

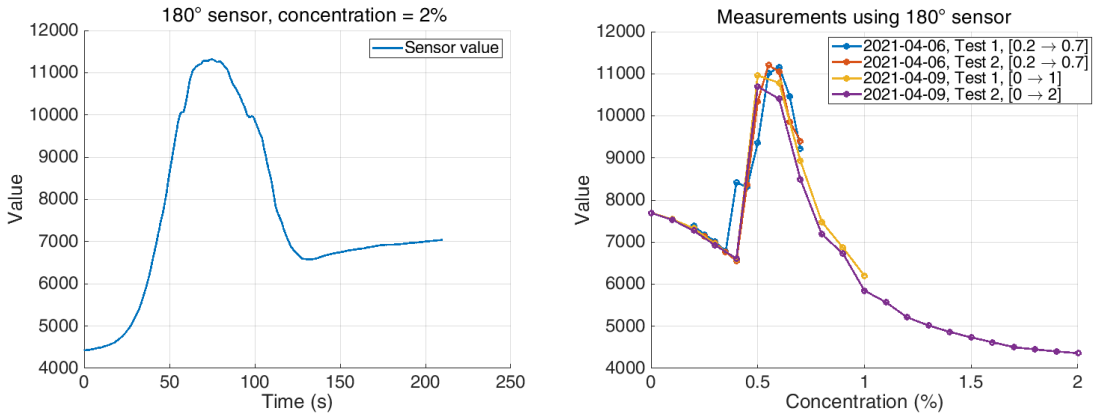

(a) *(b)*

Figure 4.24: ***(a)*** measured value from the 180° sensor during the sedimentation process. ***(b)*** Measured value from the 180° sensor for different slurry concentrations.

In Figure 4.24 its possible to observe the sedimentation process using the 190° sensor. At the start of the test (Time = 0) the sensor reading at this time is approximately 5000, which correlates to a concentration around 1.8%. The concentration then decreases and after 70s the sensor reading is around 6800 correlated to a concentration of 0.6%. The sedimentation process continues and at the ed of the test sensor value is approximately 6200 and the concentration ≈ 0.3.

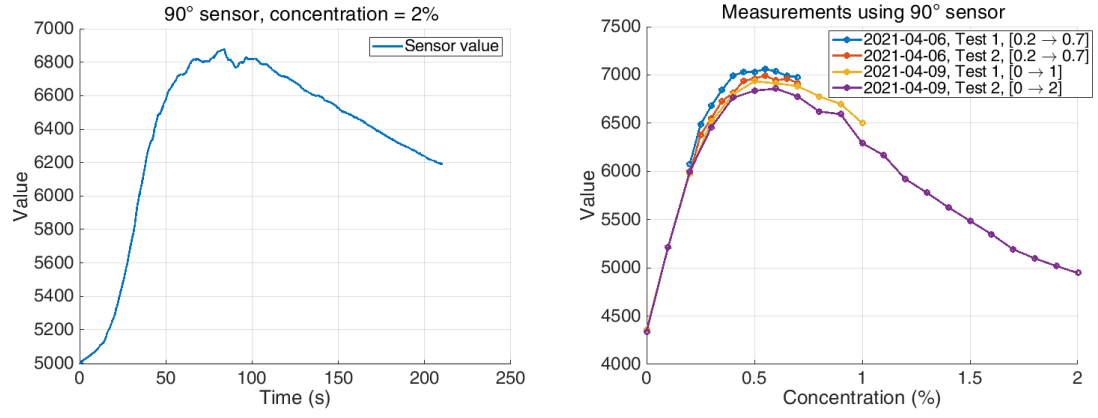

(a) *(b)*

Figure 4.25: ***(a)*** Measured value from the 90° sensor during the sedimentation process. ***(b)*** Measured value from the 90° sensor for different slurry concentrations.

In Figure 4.26 it can be observed that the measurements are affected by the sedimentation in the same way as in Figures 4.24 and 4.25.

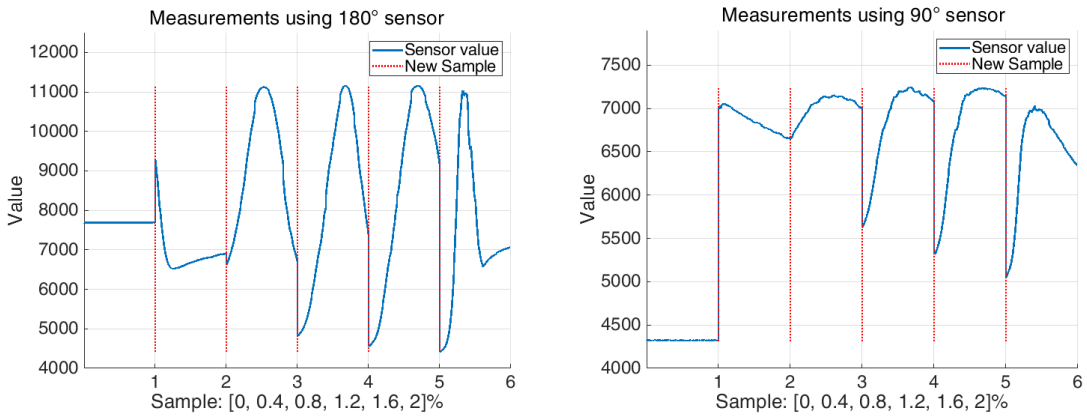

(a) *(b)*

Figure 4.26: This figure shows measurements made on slurry with a particle concentration of 0,0.4,..,2 %, using the CN0409. At each of the red vertical lines, the liquid is changed.

4.5 Measurements on filtrated slurry water

This test was performed to examine how the different sensor solutions behaved on filtered slurry with unknown concentration. The fact that the concentration is unknown after the filtration process makes it impossible to calculate an exact error. However, by comparing images of the filtered slurry and its estimated concentrations with the images of known concentrations in Figure 4.1, a rough approximation of the error can be performed.

During the test, measurements were taken on filtrated slurry that had been filtered through one of three different filter bags. The filter bags have three different mesh sizes and different numbers of layers. A description of the filter bags can be seen in Table 4.1. The filtered slurry was created by vacuuming up slurry using a wet vaccum cleaner with a filter bag installed and then taking samples from the output of the filter bag. Four samples were taken for each filter bag with the first sample, later denoted Sample 0, being on clean water going through the filter bag. Before each new filter bag, the wet vaccum cleaner was emptied and cleaned.

Both the optical sensors and the ultrasonic sensor were used to collect measurement data from the recycled slurry water. For this test, the still water test rig was used and the ultrasonic sensors were placed 60 mm apart from each other. No pump was used to circulate the recycled slurry. The test result using this setup, as well as the results using the CN0409 sensor card can be found in Section 4.5.2 to Section 4.5.4.

Table 4.1: Description of the different filter bags used in testing.

Filter bag number	Description
Filter bag 1	Finest mesh out of tested bags. 4 layers. Used in a slurry recycling, water management system.
Filter bag 2	Not as fine mesh 3 layers Used in a ordinary wet vaccum cleaner.
Filter bag 3	Fine mesh. 4 layers. Used in a ordinary wet vaccum cleaner.

4.5.1 Mapping of measurements on filtered slurry water to concentration

From the visual analysis in Section 4.1 it was estimated that the filtered slurry in a slurry recycling machine would have a concentration below 2%. The tests using the ultrasonic transducers in Section 4.2 show that the ultrasonic signal is drifting and have a low signal to noise ratio for such high concentrations. Because of this, no model for estimating the concentrations was developed.

4.5.1.1 Turbidity probe

The estimation of the concentration for the turbidity probe was done by taking an average of the first 100 sensor readings to create the received voltage V_r used in the mapping to concentration.

From Equation (2.3) and the data set of concentrations between 0% and 1.2% (seen in Figure 4.16b) the linear model

$$c = -6.7935 \cdot ln\left(\frac{V_r}{V_0}\right) - 0.0885 \tag{4.1}$$

was derived by using a MMSE estimator.

An example of a mapping can be seen in Figure 4.27, where a measurement on Sample 2 from Filter bag 3 is shown to have an estimated concentration of 0.31%. More results where this model have bean used can be found in Sections 4.5.2 to 4.5.4. If the results in Sections 4.5.2 to 4.5.4 are compared with the photos of different concentrations in Figure 4.1, it can be concluded that the turbidity probe gives a good approximation of the concentration.

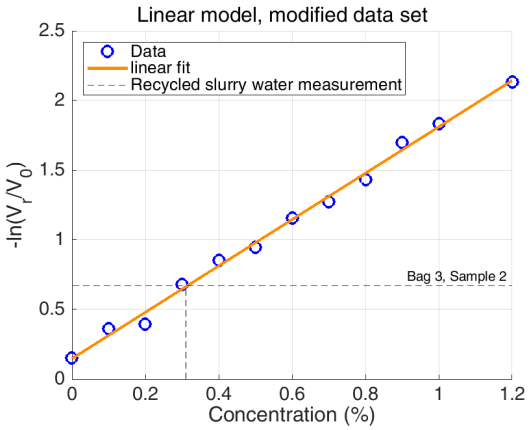

Figure 4.27: An example of mapping a measurement from the turbidity probe to a concentration using Equation (4.1).

4.5.1.2 Turbidity sensor card CN0409

In Section 4.4.3 an unexpected behavior was detected in the sensor card CN0409's 180° reading. This increase in signal strength for concentrations between 0.4 and 0.6 percent makes it problematic to map the sensor readings to a concentration. One problem that this behavior introduces is that each sensor value between 6500 and 11000 corresponds to 2-3 concentrations for the 180° sensor. This can be seen in Figures 4.28a, 4.29a and 4.30a. Since this is not the expected behavior for light transmittance and makes the mapping problem much more complex, no algorithm was developed to map a sensor reading to a concentration. However, the sensor readings in Figures 4.28 to 4.30 shows that relationship between the 90° and 180° measurement is similar to the ones on unfiltered slurry. This indicates that a mapping between sensor readings and concentration would perform similarly on both filtered and unfiltered slurry.

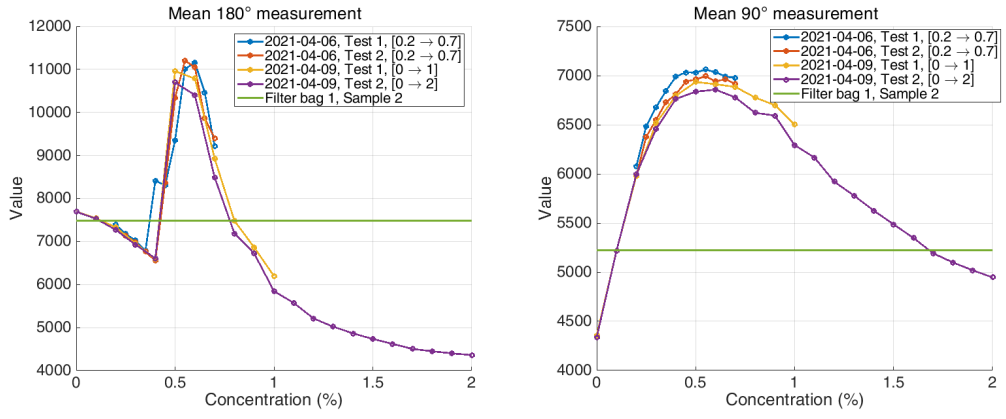

(a) *(b)*

Figure 4.28: Comparison between measurement on Filter bag 1, sample 2 and measurements of known concentration. Each value is calculated by taking the mean of the first 4 sensor readings during that measurement.

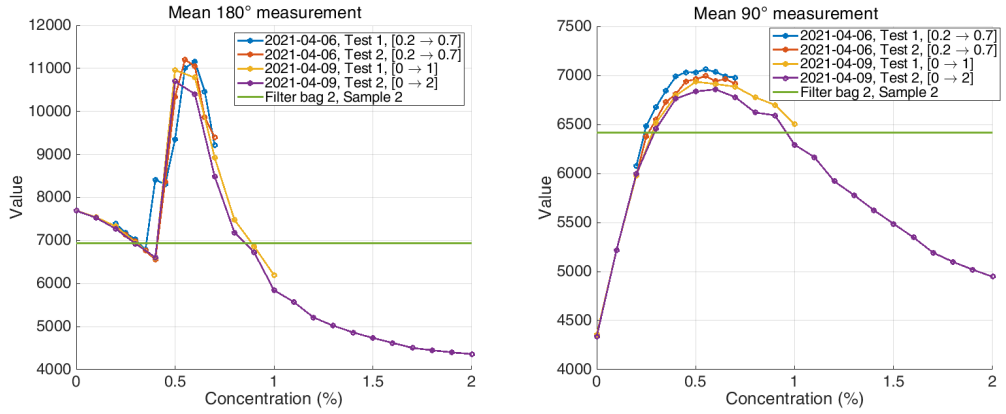

(a) *(b)*

Figure 4.29: Comparison between measurement on Filter bag 2, sample 2 and measurements of known concentration. Each value is calculated by taking the mean of the first 4 sensor readings during that measurement.

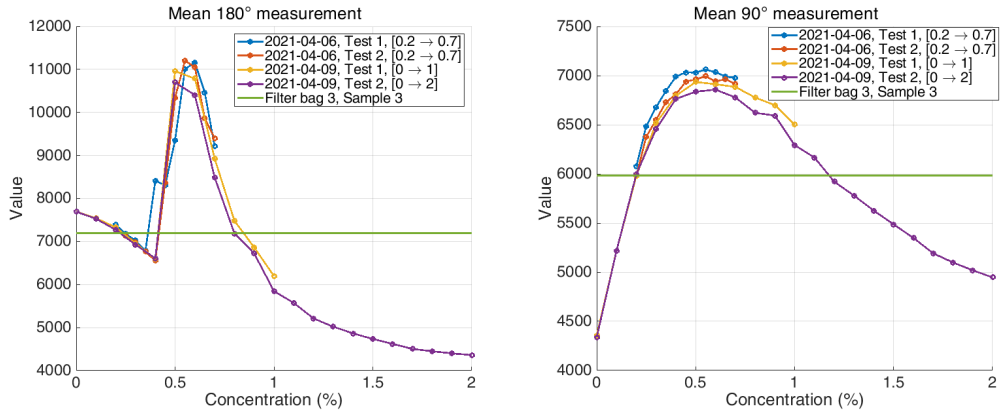

(a) *(b)*

Figure 4.30: Comparison between measurement on Filter bag 3, sample 3 and measurements of known concentration. Each value is calculated by taking the mean of the first 4 sensor readings during that measurement.

4.5.2 Measurements using Filter bag 1

Photographs of the samples taken from the filtrated slurry water using Filter bag 1 can be seen in Figure 4.31. During these tests some time passed between the vacuuming and the sampling of the filtrated slurry. This was done in order to give the slurry time to filter through the filter bag. Comparing photographs of the samples from filter bag 1 to each other, Sample 1 appears to have the highest concentration and Sample 0 the lowest. However, the color of the concrete dust and the lighting might affect the visual comparison.

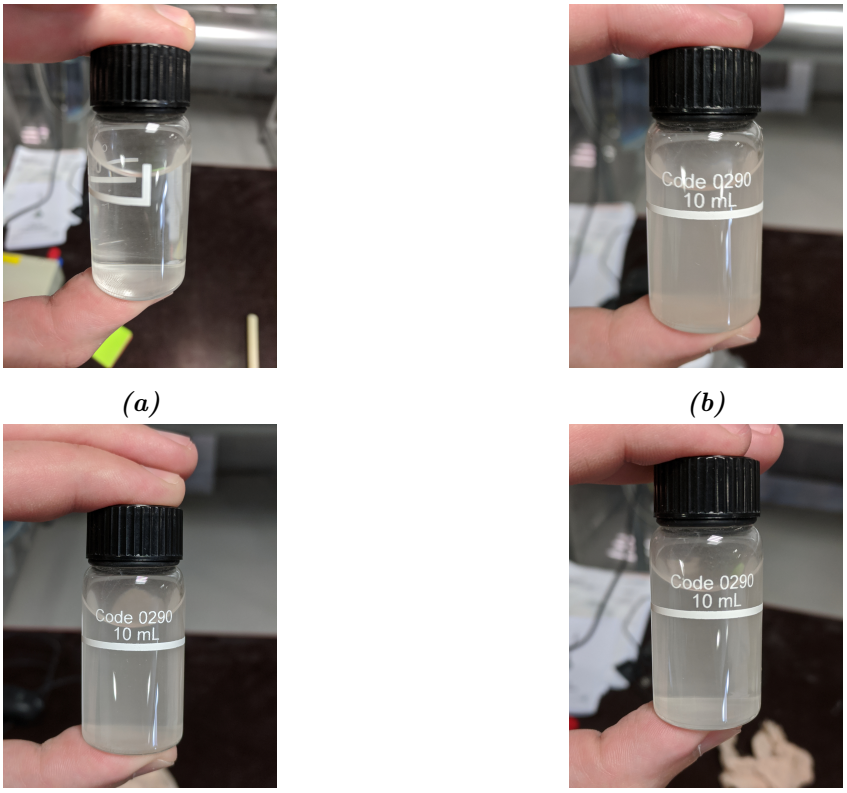

(a) *(b)* *(c)* *(d)*

Figure 4.31: Photographs of the samples taken from filtered slurry using Filter bag 1. ***(a)*** Sample 0. ***(b)*** Sample 1. ***(c)*** Sample 2. ***(d)*** Sample 3.

4.5.2.1 Ultrasonic

The ultrasonic measurements from the samples taken from filtered slurry using Filter bag 1 can be seen in Figure 4.32. The measurements have a relatively low variance. The ultrasonic measurements on Samples 1, 2 and 3 are ordered the same way as the measurements using the turbidity probe, seen in Figure 4.33. However, Sample 0 in Figure 4.32 does not correspond to the strongest ultrasonic signal. This is probably due to the drift described in Section 4.2.3. The reason that only one measurement is included for Sample 0, is because of a saving error that occurred during the test.

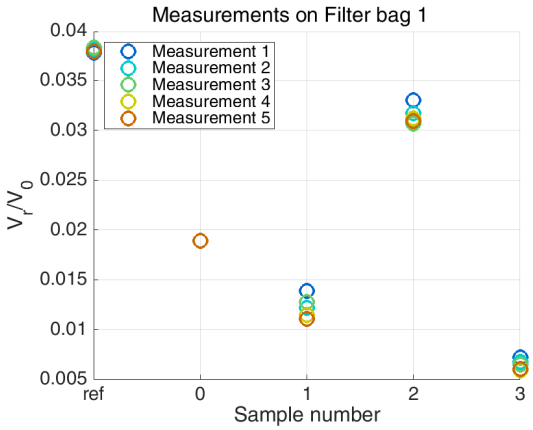

Figure 4.32: Ultrasonic measurements on the filtrated slurry water from Filter bag 1. The reference measurements (ref) were taken directly on tap water.

4.5.2.2 SEN0189 turbidity probe

The results from the measurements using turbidity probe on recycled slurry from Filter bag 1 can be seen in Figure 4.33. The measurements have a low amount of noise and show little to no effect of sedimentation for Samples 1, 2 and 3.

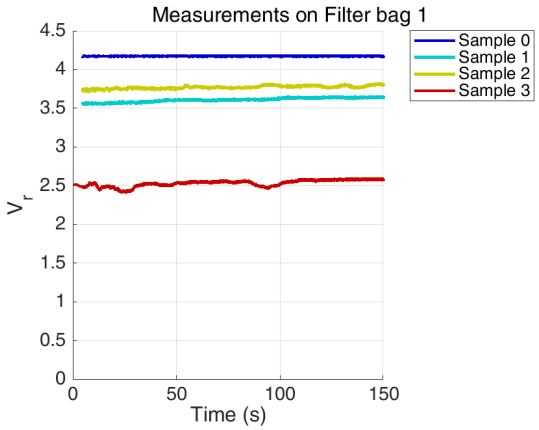

Figure 4.33: Optical measurements using the SEN0189 turbidity probe on filtrated slurry water from Filter bag 1.

The estimated concentration is calculated as described in Section 4.5.1.1, and are presented in Table 4.2. It can be observed that Sample 0 has an estimated concentration below 0%. One reason for this can be that the water used in the test is cleaner than the one used during the calibration. Another possibility is that the sensor has drifted during the weeks between the test used for calibration and this test. When comparing the estimated concentrations for the samples with their corresponding photograph in Figure 4.31, the estimations seams reasonable since all samples seem to be of low concentration. However, in Figure 4.31 it looks like Sample 1 has a higher concentration than Sample 3. This is in contrast to the estimated concentrations where Sample 3 has a higher estimated concentration than Sample 1.

Table 4.2: Table over the results for estimation of the concentration of samples from Filter bag 1.

Sample no.	V_r avg	c (%)
Sample 0	4.17	-0.04
Sample 1	3.56	0.05
Sample 2	3.74	0.02
Sample 3	2.48	0.27

4.5.2.3 CN0409

The measurements on the filtered slurry water using the sensor card can be seen in Figure 4.34. As described in Section 4.5.1.2 no model have been developed to translate the sensor reading to a concentration. However, it can be concluded that the measurements have a small noise and show little to no effect of sedimentation, for all samples.

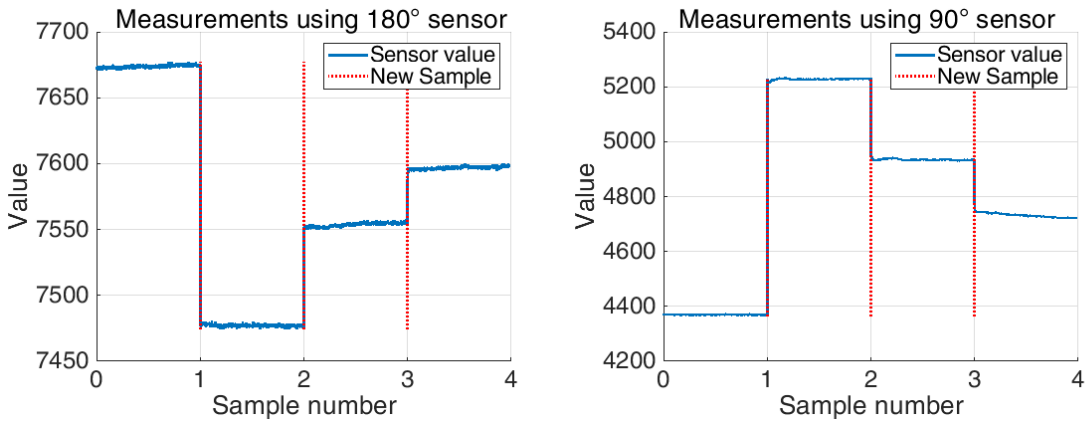

(a) ***(b)***

Figure 4.34: Optical measurements using the sensor card CN0409 on filtrated slurry water from Filter bag 1.

4.5.3 Measurements using Filter bag 2

Photographs of the samples taken from the filtrated slurry, using Filter bag 2, can be seen in Figure 4.31. The wet vaccum cleaner was cleaned, and Sample 0 was drawn directly from tap water that had passed through the wet vaccum cleaner. For Samples 1 and 2, some time passed to give the slurry time to be filtered through the filter bag. No time passed between drawing Sample 3 and vacuuming up new slurry to fill the filter bag. Comparing photographs of the samples from Filter bag 2 to each other, Sample 3 appears to have the highest concentration and Sample 0 the lowest. However, the color of the concrete dust and the lighting might affect the visual comparison.

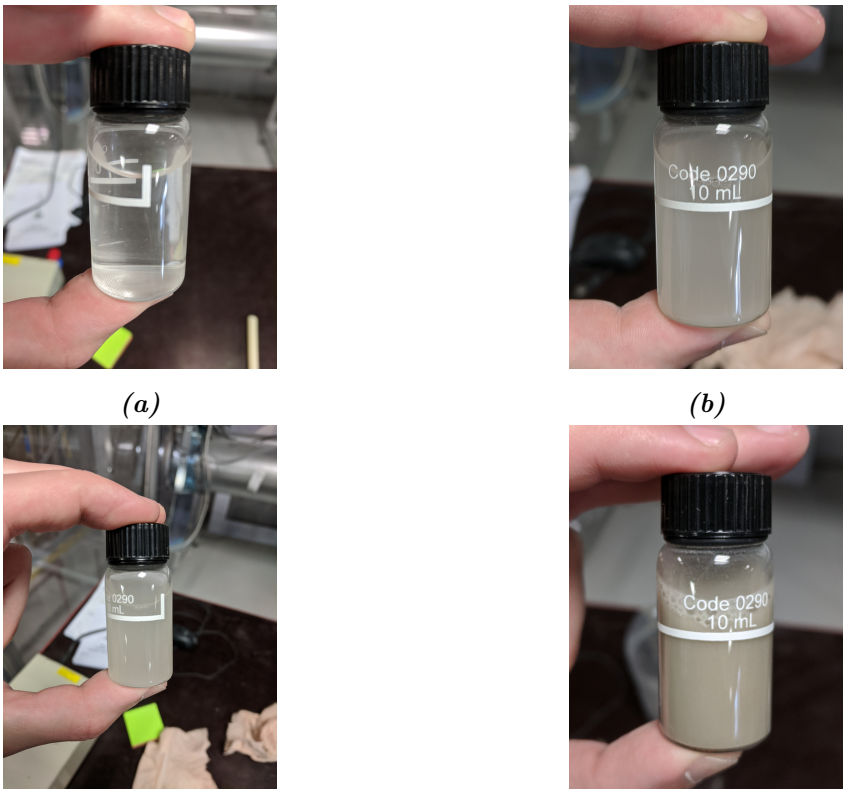

(a) *(b)* *(c)* *(d)*

Figure 4.35: Photographs of the samples taken from filtered slurry using Filter bag 2. ***(a)*** Sample 0. ***(b)*** Sample 1. ***(c)*** Sample 2. ***(d)*** Sample 3.

4.5.3.1 Ultrasonic

The ultrasonic measurements from the samples taken from filtered slurry using Filter bag 2 can be seen in Figure 4.36. The variations in the measurement seams to increase for each new sample. This can partly be explained by the noise and sedimentation seen in the turbidity probe measurements that are displayed in Figure 4.37. Note that there is only one measurement on Sample 0, this is because of a saving error that occurred during the test.

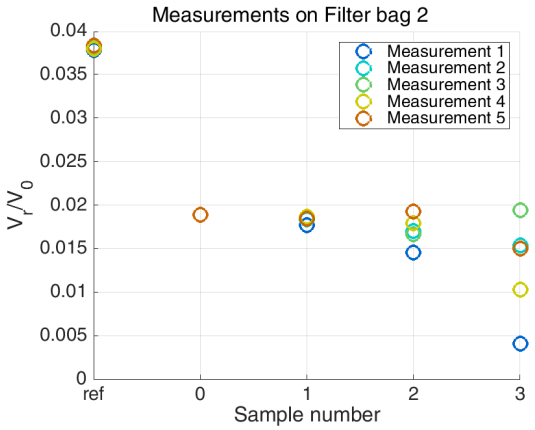

Figure 4.36: Ultrasonic measurements on the filtrated slurry water from Filter bag 2. The reference measurements, ref, were taken directly on tap water.

4.5.3.2 SEN0189

The measurements on the filtered slurry from the turbidity probe can be seen in Figure 4.37. The measurement on Samples 0 and 1 have a relatively low noise level, while the noise is more dominant in measurements on Samples 2 and 3. The sedimentation can clearly be seen in Sample 3, but is also present in Samples 1 and 2.

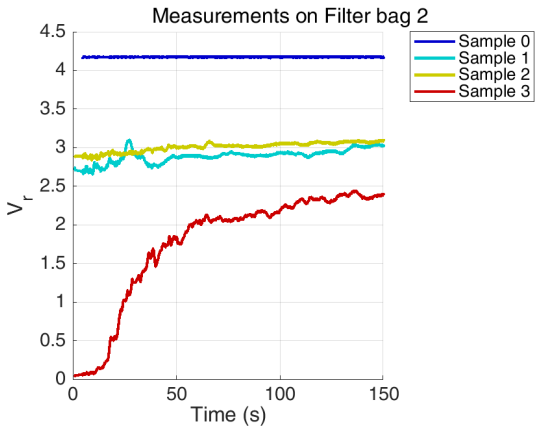

Figure 4.37: Optical measurements using the SEN0189 turbidity probe on filtrated slurry water from Filter bag 2.

The estimated concentrations are calculated as described in Section 4.5.1.1, and are presented in Table 4.3. As in the results from measurements on Filter bag 1, it can be observed that Sample 0 has an estimated concentration below 0%. One reason for this can be that the water used in the test is cleaner than the one used during the calibration. Another possibility is that the sensor has drifted during the weeks between the test used for calibration and this test. When comparing the estimations with their corresponding photograph in Figure 4.35 and the photographs of known concentrations in Figure 4.1, the estimations seem reasonable.

Table 4.3: Table over the results for estimation of the concentration of samples from Filter bag 2.

Sample no.	V_r avg	c (%)
Sample 0	4.17	-0.04
Sample 1	2.70	0.22
Sample 2	2.89	0.18
Sample 3	0.06	2.46

4.5.3.3 CN0409

The measurements on the filtered slurry water using the sensor card can be seen in Figure 4.38. The measurements have a small noise and show little to no effect of sedimentation for Samples 0, 1 and 2. However, from the measurements on Sample 3, the sedimentation is clearly visible. As described in Section 4.5.1.2 no model have been developed to translate the sensor reading to a concentration. This makes it hard to compare the measuring techniques with each other.

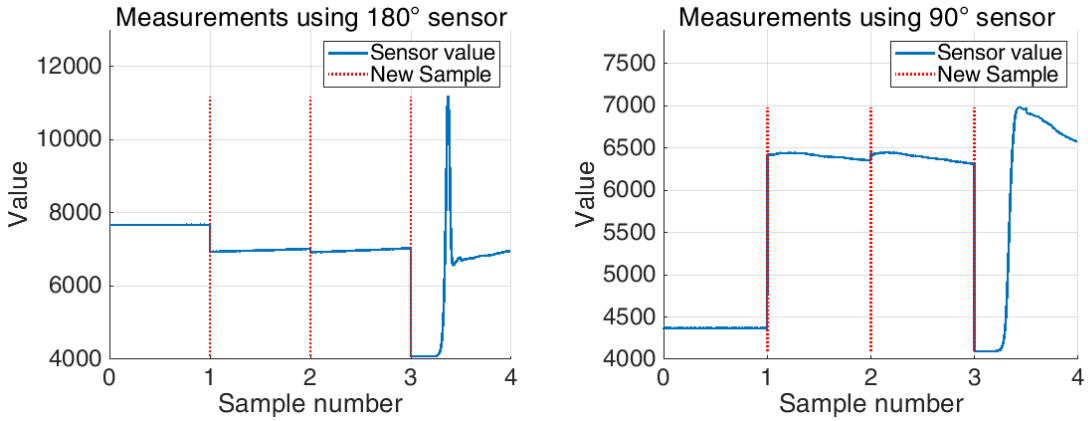

(a) *(b)*

Figure 4.38: Optical measurements using the sensor card CN0409 on filtrated slurry water from Filter bag 2.

4.5.4 Measurements using Filter bag 3

Photographs of the samples taken from the filtrated slurry, using Filter bag 3, can be seen in Figure 4.39. The wet vaccum cleaner was cleaned and Sample 0 was drawn directly from tap water that had passed through the wet vaccum cleaner. The filter bag had high flow through it, so Sample 1 was drawn directly after the slurry had been vacuumed up. It was however concluded that the time between vacuuming up the slurry and taking a sample had a large impact on the slurry concentration. For Samples 2 and 3, some time was allowed to pass before the samples were drawn. Comparing photographs of the samples from filter bag 3 to each other, Sample 3 and 2 appears to have the highest concentration and Sample 0 the lowest. Be aware that the color of the concrete dust and the lighting might affect the visual comparison.

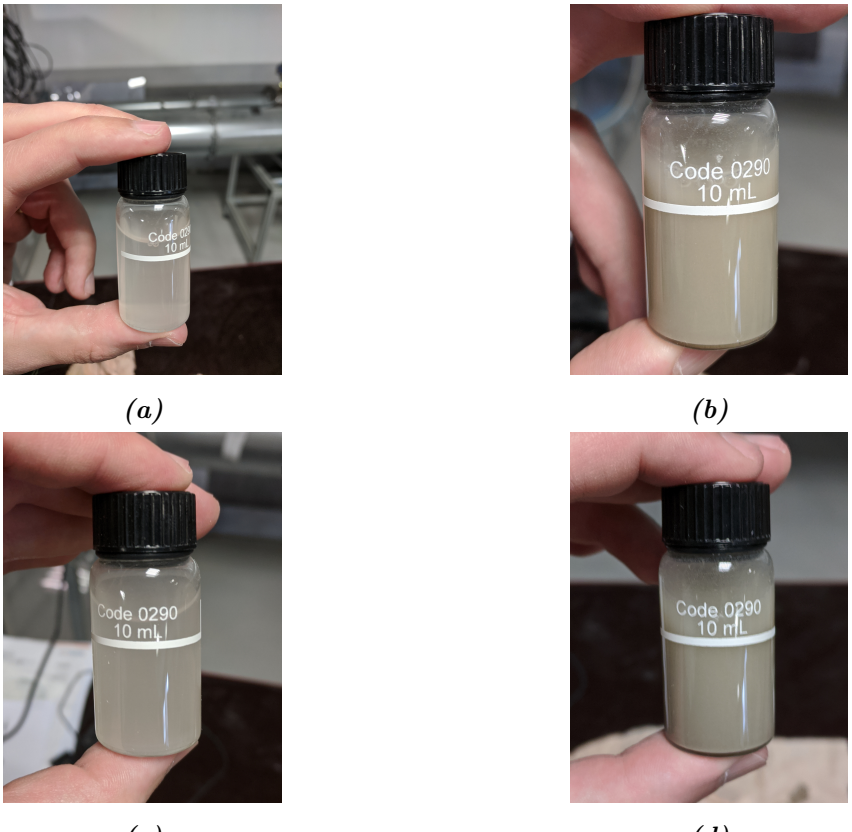

(a) *(b)* *(c)* *(d)*

Figure 4.39: Photographs of the samples taken from filtered slurry using Filter bag 3. ***(a)*** Sample 0. ***(b)*** Sample 1. ***(c)*** Sample 2. ***(d)*** Sample 3.

4.5.4.1 Ultrasonic

The ultrasonic measurements from the samples taken from filtered slurry using Filter bag 3 can be seen in Figure 4.40. When comparing the ultrasonic measurements it seems like Sample 1 has the lowest concentration. However, when the photographs of the different samples in Figure 4.39 are compared, it can be seen that both Samples 0 and 2 have a lower concentration.

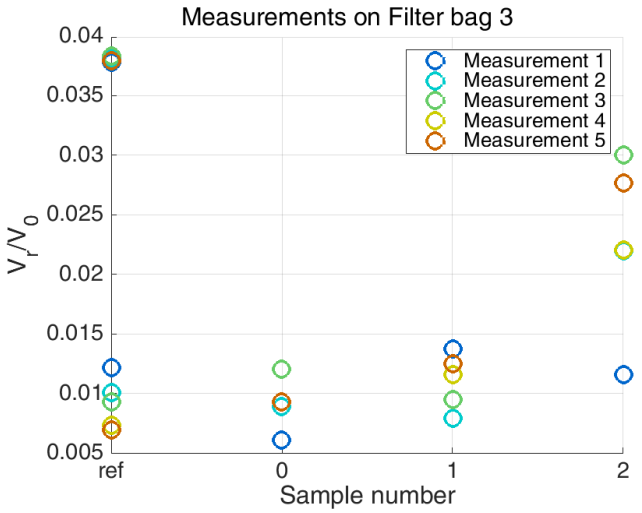

Figure 4.40: Ultrasonic measurements on the filtrated slurry water from Filter bag 3. The reference measurements, ref, were taken directly on tap water.

4.5.4.2 SEN0189

The results from the measurements using the turbidity probe on recycled slurry from Filter bag 3 are displayed in Figure 4.41. The machine was not able to be cleaned to the same degree as before the start of the previous tests, and a clear difference could be noted in the measurements on Sample 0. Therefore, the previous measurements on clean water through the machine were included as a reference. The measurement on Samples 0 and 2 have a relatively low noise level and show little to no effect of sedimentation. Samples 1 and 3 have more noise and the sedimentation process can clearly be seen in these measurements.

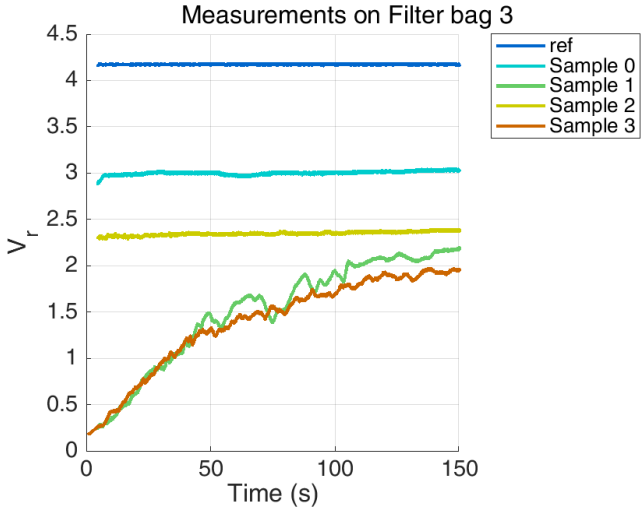

Figure 4.41: Optical measurements using the SEN0189 turbidity probe on filtrated slurry water from Filter bag 3.

The estimated concentrations are calculated as described in Section 4.5.1.1, are presented in Table 4.4. When comparing the estimations with their corresponding photograph in Figure 4.39 and the photographs of known concentrations in Figure 4.1, the estimations seem reasonable.

Table 4.4: Table over the results for estimation of the concentration of samples from Filter bag 3.

Sample no.	V_r avg	c (%)
Sample 0	2.91	0.17
Sample 1	0.27	1.60
Sample 2	2.30	0.31
Sample 3	0.26	1.63

4.5.4.3 CN0409

The measurements on the filtered slurry water using the sensor card can be seen in Figure 4.42. The sedimentation has a small impact on both Samples 0 and 2. The sedimentation process is however clearly visible in Samples 1 and 3. As described in Section 4.5.1.2 no model have been developed to translate the sensor reading to a concentration. This makes it hard to compare the measuring techniques with each other.

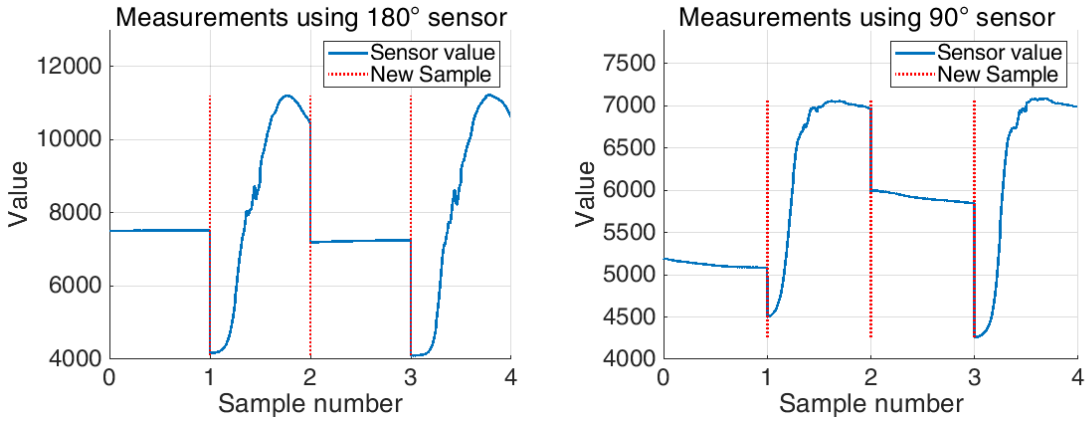

(a) ***(b)***

Figure 4.42: Optical measurements using the sensor card CN0409 on filtrated slurry water from Filter bag 3.

5
Conclusions & Discussion

This chapter will present the conclusion made from the testing of the sensors and investigation of the research questions.

The expected range of particle concentration of recycled slurry water depends on many factors. The two most important ones are how fine the mesh of the filter bag is and how much of the sedimentation process is allowed to occur in the recycling machine. By using Filter bag 1 as a reference, since it is a filter bag used in an existing slurry recycling machine, one could expect that the recycled slurry would have an approximate concentration of 0.02% to 0.3%.

5.1 Measuring on concrete slurry from different applications

According to [10, 8] there are other parameters than the concentration that affects the ultrasonic and optical measurements. Some of the other parameters that can affect the measurement are particle size, particle shape, color and viscosity. These parameters may change depending on what power tool is used, as well as the type of concrete and the amount of rebar in the sample. This is the same problem that is encountered in turbidity measurements as described in Section 2.3. Further research is needed to investigate the effect of various materials and applications have on the concentration measurement. However, the results (seen in Section 4.5.1.2) indicate that the difference between measuring on filtered and unfiltered slurry might be small.

5.2 Ultrasonic

As seen in the results from the high concentration test in Section 4.2.1, the ultrasonic measuring technique showed promising results when used on slurry concentrations of 0% to 10% with 1% increments. There are too few samples to draw any real conclusions but the results indicate that a larger distance between the transmitter and receiver leads to a higher signal to noise ratio. It can also be observed that Equation (2.5) seems to be a realistic model for concentration measurements using this technique.

When it comes to measurements on concentrations below 2% the noise and drift

of the ultrasonic signal have a huge impact on the measurement, as seen in Section 4.2.2. The change in temperature could be one of the factors causing this drift. However, the tests performed in Section 4.2.3 show that there are factors other than the temperature that affects the drift.

During the tests on flowing water, there was a problem with bubbles on the transducers. This in combination with the short distance between the transducers lead to noisy measurements. This makes any hard conclusions about the performance of the ultrasonic sensor on flowing water difficult to make, especially in a case where no bubbles were present.

5.3 Turbidity probe

As presented in the results from the high concentration test that was conducted in Section 4.3.1, the SEN0189 turbidity probe is not suited to be used in applications where it is expected that the slurry concentration is higher than 2%. Measurements on concentrations below 2% showed a good signal to noise ratio as long as the probe was placed correctly in the measuring medium. The results also show that Equation (2.3) is a good model for optical concentration measurements when the sensor is placed at 180° from the light source. The signal could also be improved using a simple moving average filter.

During the tests on flowing water, there was a problem with air bubbles forming on the sensor. This led to a noisy signal with different biases depending on the number of bubbles, making it difficult to create a model for these measurements.

5.4 CN0409

The CN0409 measures both the light at 90° and 180° from the light source. It consists of two photodiodes and two LEDs and works in two time slots to be able to negate the effect of ambient light. The CN0409 also has the possibility to perform turbidity measurements that closely resemble commercially available turbidity meters on the interval 0-1000 FTU, according to [23].

During the test on stable solutions, the CN0409 showed promising results with a high signal to noise ratio. The use of a test vial made it difficult to get stable measurements on solutions where sedimentation occurred.

A major flaw of the CN0409 is the increased sensor readings from the 180° sensor on slurry concentrations between 0.3% and 0.5%. This behavior does not seem to be limited to the CN0409 used in this project, and no comforting explanation for this has yet been found.

5.5 Which measuring technique is best suited for a slurry recycling machine?

The results from measurements on filtrated slurry water from Filter bag 1 are the most indicative of what particle concentration might be expected in recycled water from a slurry recycling machine. These results point towards that the concentration can be expected to be well beneath 2%. The test shows that for slurry concentrations below 2% the optical solutions have a high signal to noise ratio on measurements from the still water test rig. The ultrasonic method becomes unreliable because of drift and noise. When it comes to optical measuring techniques, it is clear that a single photodiode placed at a 180° angle from the light source can give a good approximation of the concentration. In theory, a better approximation could be made by measuring and combining the light intensity at both 90° and 180°. This was not implemented since the 180° measurement of the CN0409 did not behave as expected. For concentrations with turbidity below 30 NTU, it is recommended to only use the 90° measurement. After the test on filtrated slurry water, a concentration with turbidity below 30 NTU seems unlikely.

When the concentration increases, less light can pass through the slurry and at some point no light at all reaches the sensor. Even though no light can pass through the slurry, it is likely that an ultrasonic signal can. This is why the ultrasonic method is better than optical ones for high concentration of slurry.

Another thing to have in mind when comparing sensor solutions is the lifespan of the sensor. Optical solutions need to be placed in direct contact with the slurry or be separated by a transparent surface. The fast build up of sediment and constant wear from concrete particles makes the lifetime of sensors and transparent surfaces really short. The ultrasonic sensors does not need to be in direct contact with the slurry since the ultrasonic signal can pass through many types of material, including stainless steel and plastics. This significantly increases the expected lifespan of the sensor. Another factor that might impact the lifespan of the sensor is the pH level of the filtrated slurry. The pH level of the concrete slurry is around 12. This is a factor that has not been investigated in this project. Since the SEN0189 turbidity probe is an inexpensive option, the lifespan of the sensor might not be a problem if the implementation in a slurry recycling machine would allow it to be exchanged regularly.

Independent of what technique is used, it is important to note that the concentration is not the only parameter that affects the measurement. Parameters such as particle size and particle shape also have an impact on the measurement. The chosen sensor solution must thus be calibrated with regard to the application.

5.6 Filter techniques to improve performance

Testing of the SEN0189 turbidity probe on the still water test rig showed that no particular signal filter needed to be used in order to compensate for any inaccuracies in the sensor. However, the when different sources of disturbances were introduced into the measurements, such as flowing water, a moving average filter was efficient at compensating for the added noise.

The sensor card CN0409 delivered measurement with a high signal to noise ratio. Thus no extra filter was needed.

While testing the ultrasonic sensors on low concentrations there were mainly two issues that could be observed, the inaccuracies and the drift. One factor of the inaccuracies might be imperfections in the soldering to connect the piezoelectric elements with the wires. While the inaccuracies might have been able to be compensated for by increasing sample size and creating a model for sorting out outliers. However, the drift makes this problematic. The drift seems to be irregular and the source of the drift is still undetermined. If it could have been determined that the drift was caused by, for instance, a change in temperature, then this could have been accounted for in a model.

6

Improvements on test rigs and future work

The scope of this project only allowed for a broad overview of some of the optical and ultrasonic measuring techniques. This leaves lots of room for future research. During the tests, some observations were also made of how the tests could be improved.

6.1 Improvements on tests

During testing of the ultrasonic transducers, it was observed that V_0 drifted over time. This is probably caused by the function generator and a new one would be needed to test and verify this.

During the measurements using the ultrasonic transducers, the signal was measured using an oscilloscope and then manually transferred to a computer. This was time consuming and resulted in only a few measurements were taken. Automation of this process would open up the possibility of having a larger sample size with a shorter time between measurements. Implementing this would make it easier to analyze the drift and noise.

During the testing on the still water test rig, a pump was introduced to circulate the slurry. This was not a perfect solution since the pump lowered into the slurry hindered some of the slurry from being properly stirred. It would be preferable be to use a magnetic stirrer instead of a pump.

When constructing the test rig for the flowing water, the turbidity probe was accidentally glued at a bad angle. If the test rig is reconstructed, it is recommended to rotate the probe (seen in Figure 4.19) to increase the flow of slurry between the LED and photodiode.

6.2 Future work

During this project, the sensor card CN0409 was supposed to be used to test how a combination of the 90° and the 180° sensor could be used to improve the measurements. Since the 180° measurements did not behave as expected, no testing was performed regarding this issue, more research is needed.

Since the turbidity increases fast with concentration, an optical solution using backscatter could be an option for future research.

During this project, tests with known concentrations have only been done using concrete dust particles acquired from dry cutting with a mean diameter of 40 μm. In future research more tests would be needed on filtered slurry with known concentrations, to examine if the mapping between measurement and concentration differs.

This report only briefly mentions parameters that might affect the lifetime of the sensors. More research and stress testing is needed to get further insight into this area if the products are to be implemented in a slurry recycling machine.

Bibliography

[1] J. Plant, N. Voulvoulis, and K. Ragnarsdottir, *Pollutants, Human Health and the Environment: A Risk Based Approach*. Wiley, 2012. [Online]. Available: https://books.google.se/books?id=D3JS6NXez5oC

[2] G. Murtaza, M. Saqib, A. Ghafoor, W. Javed, B. Murtaza, M. K. Ali, and G. Abbas, *Climate Change and Water Security in Dry Areas*. Berlin, Heidelberg: Springer Berlin Heidelberg, 2015, pp. 1701–1730. [Online]. Available: https://doi.org/10.1007/978-3-642-38670-1_79

[3] J. Chaouki, F. Larachi, and M. Dudukovic, *Non-invasive monitoring of multiphase flows*. Elsevier, 1997.

[4] C. Yan, L.-S. Zhai, H.-X. Zhang, H.-M. Wang, and N.-D. Jin, "Cross-correlation analysis of interfacial wave and droplet entrainment in horizontal liquid-liquid two-phase flows," *Chemical Engineering Journal*, vol. 320, pp. 416–426, 2017.

[5] N. Damaschke, H. Nobach, and C. Tropea, "Optical limits of particle concentration for multi-dimensional particle sizing techniques in fluid mechanics," *Experiments in fluids*, vol. 32, no. 2, pp. 143–152, 2002.

[6] J. Carlson and A. Grennberg, "Ultrasonic measurements of particle concentration in a multiphase flow," in *1999 IEEE Ultrasonics Symposium. Proceedings. International Symposium (Cat. No.99CH37027)*, vol. 1, 1999, pp. 757–760 vol.1.

[7] G. Xu, C. Fitzpatrick, and J. Gregory, "Floc formation, size distribution, and its transformation detected by online laser particle counter," *Separation Science and Technology*, vol. 43, no. 7, pp. 1725–1736, 2008.

[8] Fondriest-Environmental. Measuring turbidity, tss, and water clarity. [Online]. Available: https://www.fondriest.com/environmental-measurements/measurements/measuring-water-quality/turbidity-sensors-meters-and-methods/

[9] M. S. Greenwood, J. L. Mai, and M. S. Good, "Attenuation measurements of ultrasound in a kaolin-water slurry. a linear dependence upon frequency," *Journal of the Acoustical Society of America; (United States)*, vol. 94:2 pt 1, 8 1993. [Online]. Available: https://www.osti.gov/biblio/6032720

[10] H. Yu, C. Tan, and F. Dong, "Measurement of particle concentration by multi-frequency ultrasound attenuation in liquid-solid dispersion," *IEEE Transactions on Ultrasonics, Ferroelectrics, and Frequency Control*, pp. 1–1, 2020.

[11] J. M. Furlan, V. Mundla, J. Kadambi, N. Hoyt, R. Visintainer, and G. Addie, "Development of a-scan ultrasound technique for measuring local particle concentration in slurry flows," *Powder Technology*, vol. 215-216, pp. 174 – 184, 2012. [Online]. Available: http://www.sciencedirect.com/science/article/pii/S0032591011005274

[12] M. Xue, M. Su, and X. Cai, "Measuring particle size and concentration of dense slurry by ultrasonic method," in *Challenges of Power Engineering and Environment*. Springer, 2007, pp. 652–655.

[13] F. Padera, "Measuring absorptance (k) and refractive index (n) of thin films with the perkinelmer lambda 950/1050 high performance uv-vis/nir spectrometers," *PerkinElmer, Inc*, 2013.

[14] A. D. McNaught, A. Wilkinson *et al.*, *Compendium of chemical terminology*. Blackwell Science Oxford, 1997, vol. 1669.

[15] C. R. Kitchin, *Stars, nebulae and the interstellar medium: observational physics and astrophysics*. CRC Press, 1987.

[16] A. Penzkofer, A. Silapetere, and P. Hegemann, "Absorption and emission spectroscopic investigation of the thermal dynamics of the archaerhodopsin 3 based fluorescent voltage sensor archon2," *International journal of molecular sciences*, vol. 21, no. 18, p. 6576, 2020.

[17] *Turbidity sensor SKU SEN0189*, DFRobot, 2020. [Online]. Available: https://docs.rs-online.com/e642/A700000007466193.pdf

[18] M. Münzberg, R. Hass, N. D. D. Khanh, and O. Reich, "Limitations of turbidity process probes and formazine as their calibration standard," *Analytical and bioanalytical chemistry*, vol. 409, no. 3, pp. 719–728, 2017.

[19] "Iso 7027-1:2016 water quality—determination of turbidity," International Organization for Standardization, Geneva, Switzerland, Tech. Rep., 2016.

[20] H. Liu, P. Yang, H. Song, Y. Guo, S. Zhan, H. Huang, H. Wang, B. Tao, Q. Mu, J. Xu *et al.*, "Generalized weighted ratio method for accurate turbidity measurement over a wide range," *Optics express*, vol. 23, no. 25, pp. 32 703–32 717, 2015.

[21] J. Krautkrämer and H. Krautkrämer, *Ultrasonic testing of materials*. Springer Science & Business Media, 2013.

[22] D. Zhang, X.-f. Gong, J.-h. Liu, L.-z. Shao, X.-r. Li, and Q.-l. Zhang, "The experimental investigation of ultrasonic properties for a sonicated contrast agent and its application in biomedicine," *Ultrasound in medicine & biology*, vol. 26, no. 2, pp. 347–351, 2000.

[23] Analog-Devices. Cn0409 circuit note. Accessed on 02.23.2021. [Online]. Available: https://www.analog.com/en/design-center/reference-designs/circuits-from-the-lab/cn0409.html#rd-documentation

[24] Arduino. analogread(). Accessed on 04.07.2021. [Online]. Available: https://www.arduino.cc/reference/en/language/functions/analog-io/analogread/

[25] G. Ghoshal, A. C. Luchies, J. P. Blue, and M. L. Oelze, "Temperature dependent ultrasonic characterization of biological media," *The Journal of the Acoustical Society of America*, vol. 130, no. 4, pp. 2203–2211, 2011.

[26] Analog Devices Inc, "Aducm360_demo_cn0409," https://github.com/analogdevicesinc/EVAL-ADICUP360/tree/master/projects/ADuCM360_demo_cn0409, 2019, commit: f68d2e0626948c24cfc18b1b4cd60683b53e16e7.

[27] rogueC. Strange readings using the 180 degree sensor on the eval-cn0409-ardz. [Online]. Available: https://ez.analog.com/circuits_from_the_lab/f/q-a/543516/strange-readings-using-the-180-degree-sensor-on-the-eval-cn0409-ardz/415649#415649

Appendices

A

Plots and images

A.1 Figures of the input voltage from testing of ultrasonic sensor

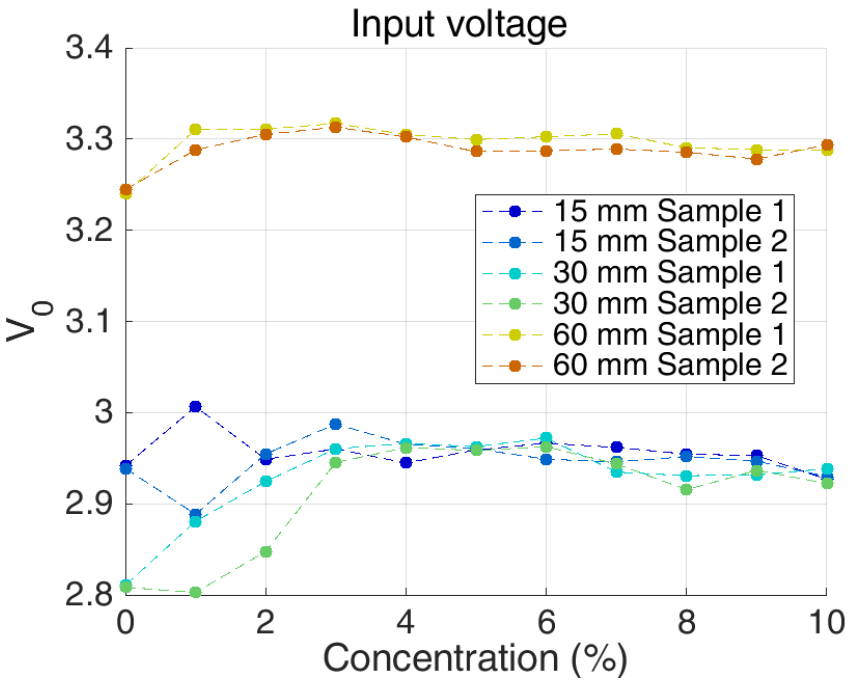

Figure A.1: The input voltage from test number one of measurements on high concentrations (0-10%).

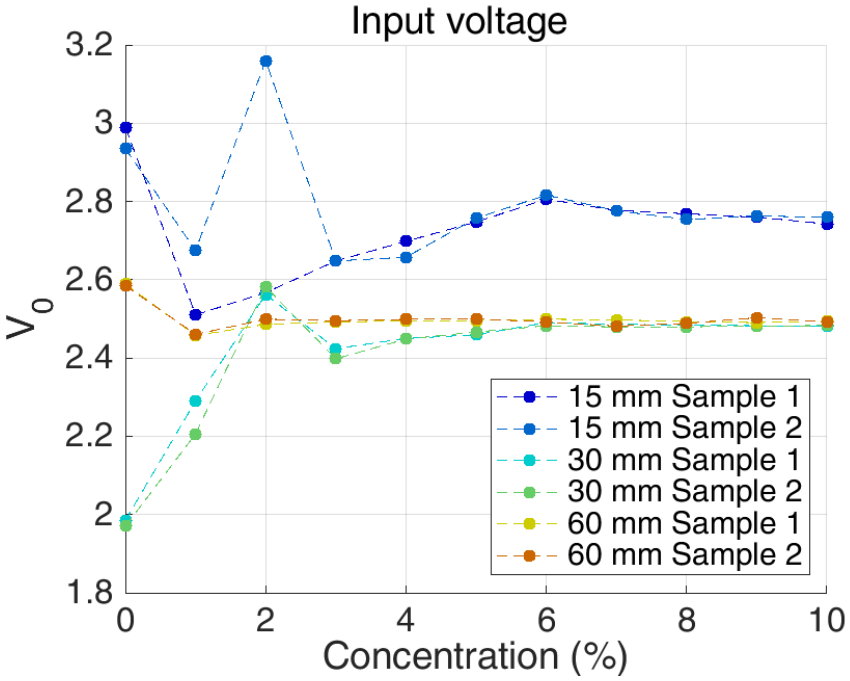

Figure A.2: The input voltage from test number two of measurements on high concentrations (0-10%).

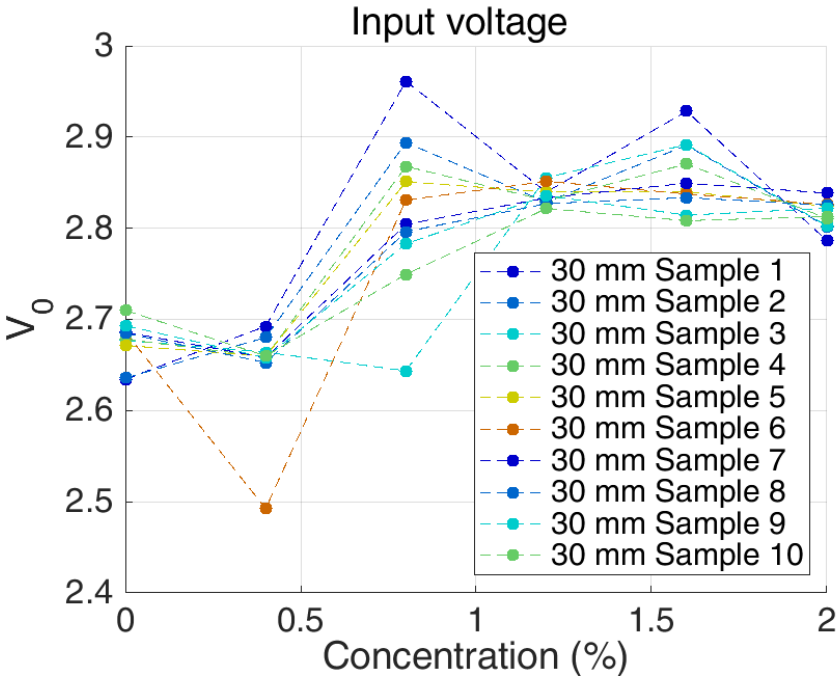

Figure A.3: The input voltage from test number one of measurements on low concentrations (0-2%).

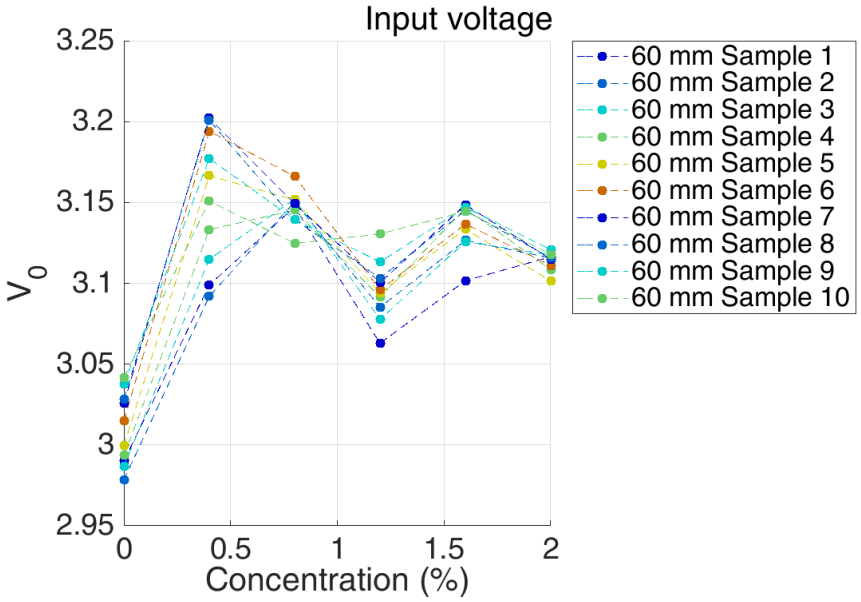

Figure A.4: The input voltage from test number two of measurements on low concentrations (0-2%).

A.2 Recycled slurry water

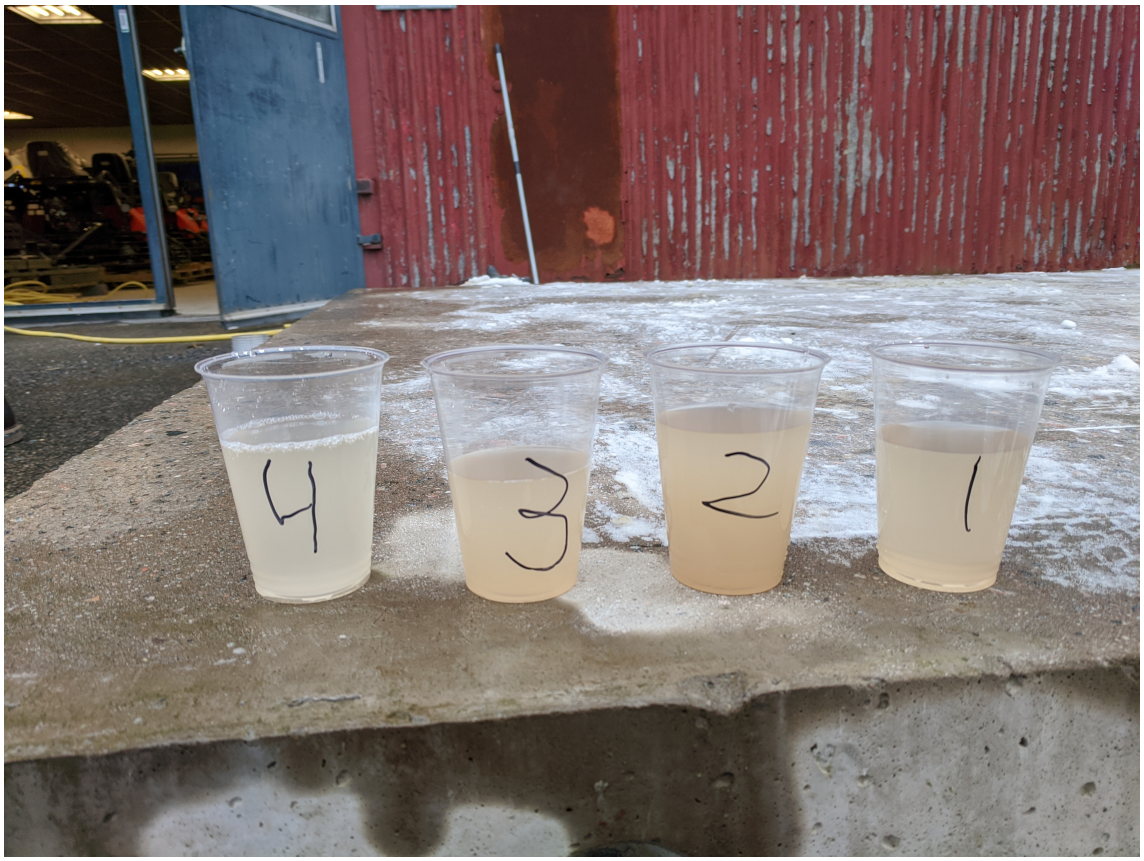

Figure A.5: Image of recycled slurry water attained from informal testing of a water management system

DEPARTMENT OF ELECTRICAL ENGINEERING
CHALMERS UNIVERSITY OF TECHNOLOGY
Gothenburg, Sweden
www.chalmers.se

CHALMERS
UNIVERSITY OF TECHNOLOGY